

AD 740575

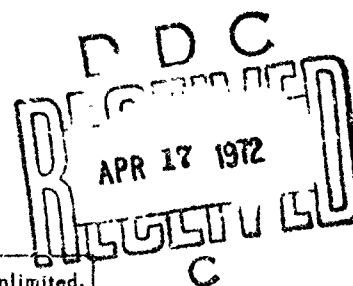
AFCRL-71-0605  
13 DECEMBER 1971  
TRANSLATIONS, NO. 95



**AIR FORCE CAMBRIDGE RESEARCH LABORATORIES**  
L. G. HANSCOM FIELD, BEDFORD, MASSACHUSETTS

**Magnetic Fields and Proton Flares--  
7 July and 2 September 1966**

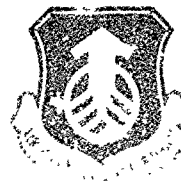
A.M. ZVEREVA  
A.B. SEVERNYI



Approved for public release; distribution unlimited.

DATE OF REVISION  
BY

**AIR FORCE SYSTEMS COMMAND**  
United States Air Force



**Unclassified**  
Security Classification

DOCUMENT CONTROL DATA - R&D		
<i>(Security classification of title, body of abstract and indexing annotation must be entered when the overall report is classified)</i>		
1. ORIGINATING ACTIVITY (Corporate author) <b>Air Force Cambridge Research Laboratories L.G. Hanscom Field Bedford, Massachusetts 01730</b>		2a. REPORT SECURITY CLASSIFICATION <b>Unclassified</b>
		2b. GROUP
3. REPORT TITLE <b>MAGNETIC FIELDS AND PROTON FLARES - 7 JULY AND 2 SEPTEMBER 1966</b>		
4. DESCRIPTIVE NOTES (Type of report and inclusive dates) <b>Scientific. Special.</b>		
5. AUTHOR(S) (First name, middle initial, last name) <b>A.M. Zvereva A.B. Severnyi</b>		
6. REPORT DATE <b>13 December, 1971</b>	7a. TOTAL NO. OF PAGES <b>76</b>	7b. NO. OF REFS <b>55</b>
8a. CONTRACT OR GRANT NO.	9a. ORIGINATOR'S REPORT NUMBER(S) <b>AFCRL-71-0605</b>	
a. PROJECT, TASK, WORK UNIT NOS. <b>N/A</b>	9b. OTHER REPORT NO(S) (Any other numbers that may be assigned this report) <b>Translations, No. 95</b>	
c. DOD ELEMENT <b>N/A</b>		
d. DOD SUBELEMENT <b>N/A</b>		
10. DISTRIBUTION STATEMENT <b>Approved for public release; distribution unlimited</b>		
11. SUPPLEMENTARY NOTES <b>TRANSLATION: Translated from Akademii Nauk SSSR. Krymskaja Astrofizicheskaja Observatorija. Izvestija. v. 41-42, pp 97-157, 1970.</b>		12. SPONSORING MILITARY ACTIVITY <b>Air Force Cambridge Research Laboratories L.G. Hanscom Field Bedford, Massachusetts 01730</b>
13. ABSTRACT <p>Longitudinal, transversal components as well as total vector of solar magnetic field in two active spot-groups produced proton-flares of 7 July and 2 Sept 1966 for the time interval before and after the flares are examined. In both cases, it was found that the field gradients <math>\Delta H_{  } / \Delta s</math> for some specific directions, the magnetic energy <math>H^2 V / 8\pi</math>, and the total magnetic flux <math>F_S + F_N</math> increase appreciably before the flares. The net flux <math>\Phi = F_S - F_N</math> through the whole active area also reaches the peak-value before the flare sometimes changing its sign. All pre-flare values are recovered after the proton flares. The change of the net magnetic flux with time, <math>\Delta \Phi / \Delta t</math>, before the examined and some other flares, leads to the emf <math>\sim 10^8</math> to <math>10^9</math> v in the fixed circuit containing the active region. It is found for important flares that this emf is about 10 times larger than emf <math>\oint [v \times H] ds</math> due to inductance, as it can be evaluated from measured velocities. Values of emf are in good agreement with the energies of protons generated by proton flares. To bring into agreement the electric currents corresponding to such emf with those measured from observed field gradients <math>j = (c/4\pi) \text{rot } H</math>, the conductivity <math>\sigma</math> should be reduced to values <math>10^8</math> to <math>10^9</math>.</p> <p>The close connection of the first appearances of flares with neutral lines <math>H_{  } = 0</math> and bifurcated regions of transverse field <math>H_{\perp}</math>, as well as the appearance of flares in the regions of higher field gradients (<math>\Delta H_{  } / \Delta s \geq 0.1</math> gs/km), have been confirmed, although some bright knots of flares appear in area of very strong longitudinal fields <math>H_{  }</math> as well as away from them, at the border of active regions. The crossing of transverse fields <math>H_{\perp}</math> peculiar and characteristic for flare regions can be connected with different levels corresponding in solar atmosphere to tubes of force crossing this region. The strength of transversal field in regions of flares can reach high values (200 to 1000 gauss).</p> <p>The process of fission of large magnetic tubes of force into smaller pieces accompanying the development of active regions is observed. No connection of flare first bright appearances either with true neutral points (<math> H  = 0</math>), or with the areas of minimal values of total strength <math> H </math> has been found. Flares appear in the regions of high field gradient <math>\Delta H_{  } / \Delta s \geq 0.2</math>, sometimes above the areas of maximal field strength <math> H </math>.</p> <p>The close connection of the bright knots of flares with the points of maximal electric current density <math>j_z</math> is found again. The map of transversal electric currents <math>j_{\perp}</math> has been obtained at first. Proton flare of 7 July 1966 appeared in the area of the junction of oppositely directed transversal currents <math>j_{\perp}</math>. A map of distribution of longitudinal electromagnetic force shows the general agreement with the distribution of the directions of line-of-sight motions. This map also indicates a possibility of oppositely directed forces acting on the middle and on the ends of flare filament.</p> <p>In conclusion, the difficulties of the neutral point's theory of flares are mentioned, as compared with the mechanism of electric current interruptions (Alfvén and Carlqvist), the possibilities of which are extended by the results of the present paper.</p>		

DD FORM 1473  
NOV 65

Unclassified  
Security Classification

Unclassified

Security Classification

14.	KEY WORDS	LINK A		LINK B		LINK C	
		ROLE	WT	ROLE	WT	ROLE	WT
	Solar flares Proton flares Solar magnetic fields						

Unclassified

Security Classification

AFCRL-71-0605  
13 DECEMBER 1971  
TRANSLATIONS, NO. 95



AFCRL RESEARCH LIBRARY

**AIR FORCE CAMBRIDGE RESEARCH LABORATORIES**

L. G. HANSCOM FIELD, BEDFORD, MASSACHUSETTS

## **Magnetic Fields and Proton Flares— 7 July and 2 September 1966**

**A.M. ZVEREVA  
A.B. SEVERNYI**

Translated from *Akademiia Nauk SSSR. Krymskaia Astrofizicheskaia  
Observatoriia. Izvestiia. V. 41-42, pp. 97-157, 1970.*

Translated by Transtek Associates, P.O. Box 339, Reading, Massachusetts 01867.

Approved for public release; distribution unlimited.

**AIR FORCE SYSTEMS COMMAND**  
**United States Air Force**



## Abstract

Longitudinal, transversal components as well as total vector of solar magnetic field in two active spot-groups produced proton-flares of 7 July and 2 Sept 1966 for the time interval before and after the flares are examined (26 records for the first and 43 for the second groups are specified in Table 1, see also Figures 4 through 10). In both cases, it was found that the field gradients  $\Delta H_{\parallel} / \Delta s$  for some specific directions (Figure 14), the magnetic energy  $H^2 V / 8\pi$ , and the total magnetic flux  $F_S + F_N$  (Figure 15) increase appreciably before the flares. The net flux  $\Phi = F_S - F_N$  (Figure 15) through the whole active area also reaches the peak-value before the flare sometimes changing its sign. All pre-flare values are recovered after the proton flares. The change of the net magnetic flux with time,  $\Delta\Phi/\Delta t$ , before the examined and some other flares, leads to the emf  $\sim 10^8$  to  $10^9$  v in the fixed circuit containing the active region. It is found for important flares that this emf is about 10 times larger than emf  $\oint [v \times H] ds$  due to inductance, as it can be evaluated from measured velocities. Values of emf are in good agreement with the energies of protons generated by proton flares. To bring into agreement the electric currents corresponding to such emf with those measured from observed field gradients ( $j = (c/4\pi)\text{rot } H$ ), the conductivity  $\sigma$  should be reduced to values  $10^8$  to  $10^9$ .

The close connection of the first appearances of flares with neutral lines  $H_{\parallel} = 0$  and bifurcated regions of transverse field  $H_{\perp}$ , as well as the appearance of flares in the regions of higher field gradients ( $\Delta H_{\parallel} / \Delta s \geq 0.1$  gs/km), have been confirmed, although some bright knots of flares appear in area of very strong longitudinal fields  $H_{\parallel}$  as well as away from them, at the border of active regions

## Abstract

(Figures 18 and 19). The crossing of transverse fields  $H_{\perp}$  peculiar and characteristic for flare regions can be connected with different levels corresponding in solar atmosphere to tubes of lines of force crossing this region (Figures 20 and 21). The strength of transversal field in regions of flares can reach high values (200 to 1000 gauss).

The process of fission of large magnetic tubes of force into smaller pieces accompanying the development of active regions is observed (Figure 23). No connection of flare first bright appearances either with true neutral points ( $|H| = 0$ ), or with the areas of minimal values of total strength  $|H|$  has been found (Figures 24 and 25). Flares appear in the regions of high field gradient  $\Delta|H|/\Delta s \geq 0.2$ , sometimes above the areas of maximal field strength  $|H|$ .

The close connection of the bright knots of flares with the points of maximal electric current density  $j_z$  is found again (Figures 26 and 27). The map of transversal electric currents  $j_{\perp}$  has been obtained at first. Proton flare of 7 July 1966 appeared in the area of the junction of oppositely directed transversal currents  $j_{\perp}$ . The map of distribution of longitudinal electromagnetic force (Figure 29) shows the general agreement with the distribution of the directions of line-of-sight motions. This map also indicates a possibility of oppositely directed forces acting on the middle and on the ends of flare filament.

In conclusion, the difficulties of the neutral point's theory of flares are mentioned, as compared with the mechanism of electric current interruptions (Alfvén and Carlqvist, 1967), the possibilities of which are extended by the results of the present paper.

## Contents

1. COMPARISON OF SIMULTANEOUS FIELD RECORDINGS IN THE VERY SAME LINE WITH TWO PHOTOMETERS	1
2. DATA OF OBSERVATIONS, MAGNETIC FIELD MAPS, GENERAL CHARACTER OF MAGNETIC CONFIGURATIONS	6
3. VARIATION OF THE LONGITUDINAL AND TRANSVERSAL FIELDS (GRADIENTS, FLUXES, FIELD ENERGY)	21
4. POSITION OF FLARES RELATIVE TO THE LONGITUDINAL AND TRANSVERSAL MAGNETIC FIELDS	36
5. PROTON FLARES AND TOTAL FIELD STRENGTH	47
6. PROTON FLARES AND ELECTRIC CURRENTS. AMPERE FORCE AND RADIAL VELOCITIES	52
7. CONCLUSIONS	60
ACKNOWLEDGMENTS	65
REFERENCES	67

## Illustrations

1. Comparison of Values of Longitudinal Field Strengths in $\lambda 5250$ Recorded Simultaneously on Two Magnetograph Channels	4
2. Comparison of the Meudon and of the Crimean Maps of the Magnetic Field $H_{\parallel}$ on 5 July 1966	5
3. Comparison of Vectors of Transversal Oscillations of $\delta_{\perp}$ Simultaneously Measured on Two Channels but at the One and Same Line, $\lambda 5250$ , on 2 Sept 1966	7
4. Isogauss Maps of the Longitudinal Field $H_{\parallel}$ for 5 July 1966 and of Signals of the Transversal Field $\delta_{\perp}$	8
5. Isogauss Maps of the Longitudinal Field $H_{\parallel}$ for 6 July 1966 and of Signals of the Transversal Field $\delta_{\perp}$	9
6. Isogauss Maps of the Longitudinal Field $H_{\parallel}$ for 7 July 1966 and of Signals of the Transversal Field $\delta_{\perp}$	10
7. Isogauss Maps of the Longitudinal Field $H_{\parallel}$ for 30 Aug 1966 and of Signals of the Transversal Field $\delta_{\perp}$	11
8. Isogauss Maps of the Longitudinal Field $H_{\parallel}$ for 31 Aug 1966 and of Signals of the Transversal Field $\delta_{\perp}$	12
9. Isogauss Maps of the Longitudinal Field $H_{\parallel}$ for 1 Sept 1966 and of Signals of the Transversal Field $\delta_{\perp}$	13
10. Isogauss Maps of the Longitudinal Field $H_{\parallel}$ for 2 Sept 1966 and of Signals of the Transversal Field $\delta_{\perp}$	14
11. Comparison of the Isogauss Maps for $\lambda 5250$ and $\lambda 6103$ for One Day	18
12. (a) Comparison of the Directions of the Transverse Fields $H_{\perp}$ for the Same Day on July 1966 in Different Lines; (b) Comparison of Directions of $H_{\perp}$ for the Same Line on Different Days (July 5, 6, and 7)	20
13. Distribution of the Strength of the Longitudinal Field $H_{\parallel}$ Along the Straight Line Connecting Hills of Different Polarities for Various Days for the First and Second Active Regions	22
14. Behavior of the Average Gradients of the Field $\Delta H_{\parallel} / \Delta S$ with Time for Certain Characteristic Directions for the First and Second Active Regions	23
15. Variations of the Magnetic Energy of the Absolute Field $ H ^2 V / 8\pi$ and of the Longitudinal Field $H_{\parallel}^2 V / 8\pi$ with Time	24
16. Behavior of the Magnetic Energy of the Longitudinal Field $H_{\parallel}^2 V / 8\pi$ of the Total Flux $F_S + F_N$ and the Resulting Flux $F_S - F_N$ with Time for the 22 June 1962 Flare	27
17. Behavior of the Total Flux $F_S + F_N$ and Resulting Flux $F_S - F_N$ for the 16 July 1969 Flare	28
18. Comparison of the Maps of the Longitudinal $H_{\parallel}$ and Transversal $H_{\perp}$ Fields With Locations of Flares for 6 and 7 July 1966	40
19. Same as in Figure 18 for 31 Aug and 1 and 2 Sept 1966	41
20. Histograms of the Locations of Bright Knots of Flares in the First and Second Active Regions Relative to the Neutral Line $H_{\parallel} = 0$	42

## Illustrations

21. Diagram of the Possible Location of the Lines of Force in the Region of Bifurcation, 6 July 1966	44
22. Comparison of the $H_{\perp}$ Directions with Fine Structure of the Spot	45
23. Example of Maps of Total Strength $ H $ at Different Lines for the First Active Groups	48
24. Location of the Flares of July 6 and 7, 1966 on the Maps of Total Intensity $ H $	49
25. Locations of Flares of 31 Aug and 2 Sept 1966 on the Maps of Total Intensity $ H $	50
26. Map of Electric Currents $j_z$ for July 6 and 7 and Location of the Flares on Them	53
27. Location of the Flares on the Maps of $j_z$ for the Second Active Region	55
28. Map of Transversal Fields $j_{\perp}$ for July 7 and Location on It of Clouds of the A and B Proton Flares	58
29. Location of Proton Flare on the $F_7$ Map for July 7	59

## Magnetic Fields and Proton Flares — 7 July and 2 September 1966

### 1. COMPARISON OF SIMULTANEOUS FIELD RECORDINGS IN THE VERY SAME LINE WITH TWO PHOTOMETERS

This paper deals with magnetic fields associated with proton flares on 7 July and 2 Sept 1966. Preliminary results of the study of the proton flare of July 7 are presented in the works of Severnyi (1968). Longitudinal  $H_{\parallel}$  and transversal  $H_{\perp}$  fields of the active spot groups, which gave rise to proton flares on 7 July and 2 Sept 1966, were recorded systematically every day, usually several times a day, on a dual magnetograph CrAO (described in the works of Severnyi, 1966). Twenty-six recordings of  $H_{\parallel}$  and  $H_{\perp}$  were obtained for the first flare and forty-three for the second. All recording data are combined in Table 1. Differently from the flare of July 7, recordings for the second active region were made on two photometers in the one and same line,  $\lambda 5250$ . These two independent recordings at the same line do in principle increase the reliability of results since both channels are practically independent, even though they are subjected to equal effects of the picture quality and scanning errors.

For appropriate focussing of recordings on both channels,  $H_{\parallel}$  as well as  $H_{\perp}$  correspond qualitatively; quantitative differences (strength values) do not exceed 15 to 20%. This is shown in Figure 1 where the strengths of the longitudinal field

---

(Received for publication 13 December 1971)

Table 1

Date 1966	Time of Recording UT		$\lambda, \text{\AA}$	Photo- meter	Field	ATT <sub>3</sub>	$\beta$ Gradient	Calibration			
	Begin- ning	End						Time	Kick E-W, mm	ATT <sub>K</sub>	1 Unit, gs.
July 4	06.05	06.30	6103	Red		200	—	06.00	102	800	2.65
	08.20	08.45	5250	Green		5000	—	08.00	84	1000	3.21
	08.20	08.45	6103	Red		200	—	08.00	140	600	2.60
July 5	06.00	06.50	5250	Green		1000	—	05.45	143	3000	3.70
	06.00	06.50	6103	Red		200	—	05.45	189	500	2.30
	08.00	08.30	5250	Green		300	—	05.45	429	3000	3.36
	08.00	08.30	5250	Green	⊥1	800	44	05.45	143	3000	—
	08.00	08.30	5250	Green	⊥2	800	44	05.45	143	3000	—
	08.35	10.10	5250	Green	⊥2	500	44	05.45	162	3000	—
	08.35	10.10	5250	Green	⊥1	500	44	05.45	162	3000	—
	08.35	10.10	5103	Red	⊥2	100	44	05.45	156	600	—
	08.35	10.10	6103	Red	⊥1	100	44	05.45	156	600	—
July 6	05.00	05.45	5250	Green		500	—	04.35	125	1000	6.40
	05.00	05.45	6103	Red		100	—	04.35	97	300	3.74
	05.48	06.25	5250	Green		500	—	04.35	125	1000	6.40
	05.48	06.25	6103	Red		100	—	04.35	97	300	3.74
	07.10	07.45	6103	Red	⊥1	200	45	06.25	204	500	—
	07.10	07.45	6103	Red	⊥2	200	45	06.25	204	500	—
July 7	05.10	05.30	5250	Green		500	—	—	152	2000	2.63
	05.10	05.30	6103	Red		100	—	05.00	116	500	1.87
	06.20	06.30	4808	Green		250	—	06.00	136	1000	21.6
	06.20	06.30	4808	Green	⊥1	400	45	06.00	136	1000	—
	06.20	06.30	4808	Green	⊥2	400	45	06.00	136	1000	—
	06.30	06.45	4808	Green		250	—	06.00	136	1000	21.6
	06.30	06.45	4808	Green	⊥1	400	45	06.00	136	1000	—
	06.30	06.45	4808	Green	⊥2	400	45	06.00	136	1000	—
	09.08	09.30	5250	Green		500	—	09.00	136	2000	9.24
	09.08	09.30	5250	Green	⊥1	500	45	09.00	136	2000	—
	09.08	09.30	5250	Green	⊥2	500	45	09.00	136	2000	—
	09.33	10.00	5250	Green		500	—	09.00	136	2000	9.24
	09.33	10.00	5250	Green	⊥1	500	45	09.00	136	2000	—
	09.33	10.00	5250	Green	⊥2	500	45	09.00	136	2000	—
10.00	10.30	5250	Green		500	—	09.00	136	2000	9.24	
10.00	10.30	5250	Green	⊥1	500	45	09.00	136	2000	—	
10.00	10.30	5250	Green	⊥2	500	45	09.00	136	2000	—	
Aug 24	14.00	14.55	5250	Green		1000	—	—	92	2000	1.76
Aug 25	06.15	10.20	5250	Green		2000	—	06.10	96	2000	3.32
Aug 26	10.35	11.45	5250	Green	⊥1	500	61	12.10	94	2000	—
	10.35	11.45	5250	Red	⊥1	25	61	12.10	54	100	—
	11.45	14.15	5250	Green	⊥2	500	61	12.10	94	2000	—
	11.45	14.15	5250	Red	⊥2	25	61	12.10	54	100	—
	14.15	15.30	5250	Green		500	—	14.15	125	1000	1.26
Aug 27	14.15	15.30	5250	Red		25	—	15.30	43	500	—
	14.15	15.30	5250	Red		25	—	14.15	65	25	3.46
	14.15	15.30	5250	Red		25	—	15.30	24	—	—
Aug 27	06.32	09.10	5250	Green		1500	—	06.25	77	4000	1.39
	06.32	09.10	5250	Red		60	—	06.50	158	1500	—
	06.32	09.10	5250	Red		60	—	06.25	85	60	2.78
								07.50	97		

Table 1. (Contd)

Date 1966	Time of Recording UT		$\lambda, \text{\AA}$	Photo- meter	Field	ATT <sub>3</sub>	$\beta$ Gradient	Calibration			
	Begin- ning	End						Time	Kick E-W, mm	ATT <sub>K</sub>	1 Unit, gs.
Aug 29	12.00		5250	Green		2000	—	11.30	137	2000	1.78
Aug 30	05.30	06.00	5250	Green		2000	—	05.00	72	2000	2.55
	05.30	06.00	5250	Red		50	—	06.10	123		
Aug 31								05.00	37	100	2.98
								06.10	94	50	
								07.20	152	2000	—
								07.20	152	2000	—
								11.35	110	3000	1.50
								11.40	101	3000	1.65
								11.40	104	100	1.55
								11.40	101	3000	—
								11.40	104	100	—
								11.40	101	3000	—
								11.40	101	3000	—
								11.40	104	100	—
								11.40	104	100	—
								11.40	104	100	—
	Aug 31	05.35	06.35	5250	Green		2000	—	05.30	120	2000
10.00		10.43	5250	Green	⊥1	500	29	09.50	90	2000	—
10.00		10.43	6103	Red	⊥1	30	29	09.50	99	80	—
10.43		11.30	5250	Green	⊥2	500	29	09.50	90	2000	—
10.43		11.30	6103	Red	⊥2	30	29	09.50	99	80	—
11.32		12.03	5250	Green		2000	—	12.03	61	2000	4.36
11.32		12.03	5250	Red		80	—	12.03	91	80	2.93
13.10		13.50	5250	Green		1000	—	13.10	74	1000	3.87
								13.50	64		
								13.10	86	80	3.34
								13.50	74		
								13.50	64	1000	4.60
								14.25	52		
								14.45	215	1000	—
								14.45	57	80	—
							14.45	215	1000	—	
							15.30	97	20	—	
Sept 1	06.00	06.40	5250	Green		4000	—	05.45	115	4000	2.47
								06.40	119		
	06.40	07.00	5250	Green	⊥1	4000	40	06.40	119	4000	—
	06.40	07.00	5250	Red	⊥1	100	40	06.40	147	100	—
	07.00	07.30	5250	Green	⊥2	4000	40	07.50	77	4000	—
	07.00	07.30	5250	Red	⊥2	100	40	06.40	147	100	—
	08.07	08.30	5250	Green	⊥2	2000	60	07.50	77	4000	—
	08.07	08.30	6103	Red	⊥2	50	60	07.50	107	100	—
	08.30	08.50	5250	Green	⊥1	2000	60	08.50	153	2000	—
	08.30	08.50	6103	Red	⊥1	50	60	08.50	231	50	—
	08.50	10.00	5250	Green		4000	—	08.50	153	2000	2.90
	10.20	10.50	5250	Green		2000	—	10.10	161	2000	2.00
								10.15	77	4000	—
								10.10	62	200	2.59
								10.15	77	4000	2.43
							10.10	62	200	2.59	
							11.20	220	50	—	

Table 1. (Contd)

Date 1966	Time of Recording UT		$\lambda, \text{\AA}$	Photo- meter	Field	ATT <sub>3</sub>	$\beta$ Gradient	Calibration			
	Begin- ning	End						Time	Kick E-W, mm	ATT <sub>K</sub>	1 Unit, gs.
Sept 2	06.00	07.15	5250	Green		2000	—	06.00	143	2000	2.31
	06.00	07.15	5250	Red		60	—	06.00	145	60	2.26
	08.50	09.25	5250	Green		8000	—	09.25	129	8000	2.55
	08.50	09.25	5250	Red		100	—	09.25	86	100	3.80
	10.55	11.30	5250	Green	⊥2	2000	59	09.25	129	8000	—
	10.55	11.30	5250	Red	⊥2	20	59	09.25	86	100	—
	11.30	12.00	5250	Green	⊥1	2000	59	09.25	129	8000	—
	11.30	12.00	5250	Red	⊥1	20	59	09.25	36	100	—

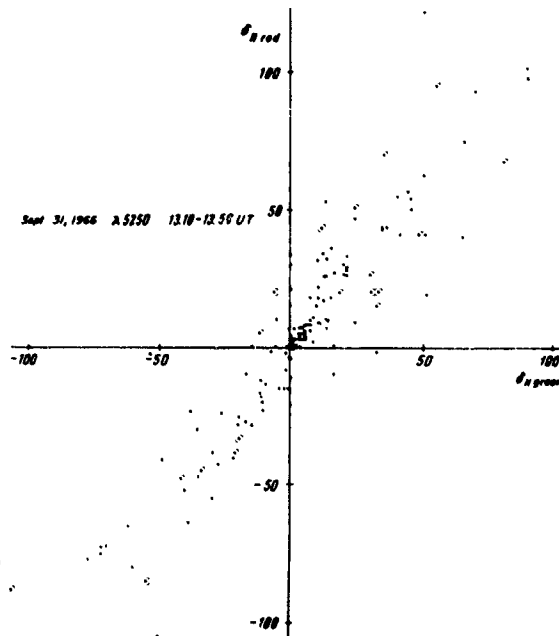


Figure 1. Comparison of Values of Longitudinal Field Strengths in  $\lambda 5250$  Recorded Simultaneously on Two Magnetograph Channels

$H_{||}$  are compared for the one and same scan in  $\lambda 5250$  on both photometers ("green" and "red"). Another evidence of the reliability of performed recordings and maps of  $H_{||}$  can be provided by the comparison of our maps with the isogauss maps obtained at the Meudon's Observatory and constructed by means of a lambdameter\* (Figure 2). We witness a good agreement between the Crimean and Meudon's maps. Quantitative difference appears when we utilize actual strength of the longitudinal magnetic field as it is determined by the empirical calibration curve of signals  $\delta_{||}$  obtained in the

\*Maps for five days were kindly offered to us by Professor P. Michard.

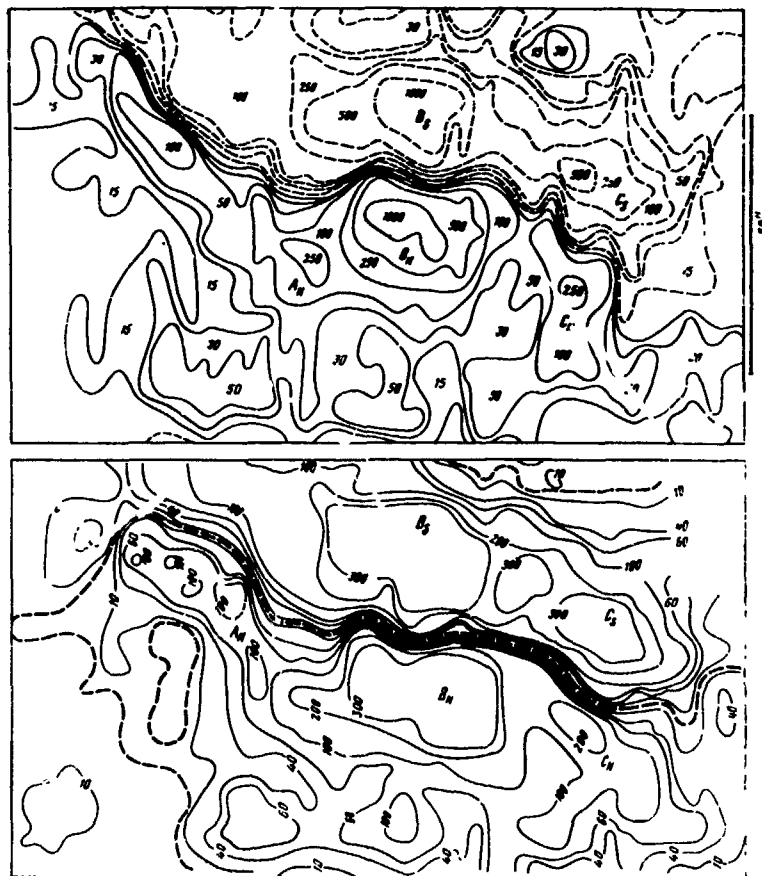


Figure 2. Comparison of the Meudon (on top: S-polarity = dashed lines; N-polarity = solid lines) and of the Crimean (at the bottom: S-polarity = vertical numbers; N-polarity = horizontal numbers; thick dashed = neutral line) Maps of the magnetic field  $H_{\parallel}$  on 5 July 1966

works of Severnyi (1967) instead of strength proportional to the magnetograph signal according to the relation

$$\delta_{\parallel} = \frac{\partial I_{\lambda}}{\partial \lambda} \Delta \lambda_{H}.$$

This difference appears for values  $H_{\parallel} > 100$  gs. If we had utilized these values uncorrected (for the saturation effect) and denoted everywhere further on the maps, then the maximum strength would not exceed 500 gs, while in the spots, it is considerably above 1000 gs, and correspondingly the energy value of the active region

(see Sec. 3) would barely reach the value necessary for the formation of a flare with an energy loss of the order of  $10^{31}$  to  $10^{32}$  ergs.

Comparison of the maps of directions and vector magnitudes of transversal oscillations  $\delta_{\perp}$  (see the example for Sept 2 on Figure 3) for simultaneous recording at the one and same line,  $\lambda 5250$ , also allows us to estimate the reliability of measurements of the azimuth of the transversal oscillation vector. Thus, for Sept 1, the differences in directions were greater than 30 to 40 deg, and occur in 10 cases out of 143, that is, in 7% of the cases. Only in one case (0.7%) does the deviation reach 60 deg. The second analogous comparison (154 cases) was made for maps of  $\delta_{\perp}$  on Sept 2 (Figure 3). It gives 8.5% for deviations greater or equal to 30 to 40 deg, and 2% for deflections greater or equal to 60 deg.

Further, on July 30 and 31, such recordings were made on purpose, such that following simultaneous recording of three components ( $H_{\parallel}$ ,  $H_{\perp 1}$ , and  $H_{\perp 2}$ ) in  $\lambda 5250$ , individual recordings of these components were performed on the same photometer in order to expose possible systematical differences between the two recording methods. They can occur because in the first case, polarization condition modulation takes place at a frequency of 22 Hz, and the velocity compensator (flat parallel plate) keeps the line in a certain intermediate state (fixed between positions  $1/4 \lambda$ -plate for  $H_{\perp 1}$  and  $H_{\perp 2}$ ). In the second case the velocity compensator keeps the line in these extreme positions corresponding to the direction of the  $1/4 \lambda$ -plate axis at a 45-deg angle to the direction of the ADP axis and the direction of this axis, coinciding with the ADP axis (see Bruns et al., 1964). Comparison has shown that differences between both methods of recording are practically nonexistent. Even if they were present, they would then be within the limits of errors characteristic for simultaneous recordings of the one and same line on the two photometers.

These results are quite significant for judging the accuracy of recordings of transversal magnetic fields because of the previously found effect of rotation of the vector of transversal oscillations during the passage from one line to the other and within the limits of the one and same line (Severnyi, 1964a). Since at the individual locations (basically at the boundary of the spots) this rotation substantially exceeds 60% (see Sec. 2), it does not seem possible to relate this effect (Severnyi, 1964a) to accidental errors.

## 2. DATA OF OBSERVATIONS. MAGNETIC FIELD MAPS, GENERAL CHARACTER OF MAGNETIC CONFIGURATIONS

Scanning of the active region (usually of a size of  $\sim 100 \times 150$  arc s) was carried out, as usual, with a distance between scans along  $\delta$  equal to 6.25 arc s (the units of length along the vertical and horizontal are equal and indicated on the maps of Figures 4 through 10), and resolution size of the slit 2.5 arc s (along  $\alpha$ )  $\times$  4.5 arc s or 9 arc s (along  $\delta$ ) which gives a continuous, without intermission, coverage of the

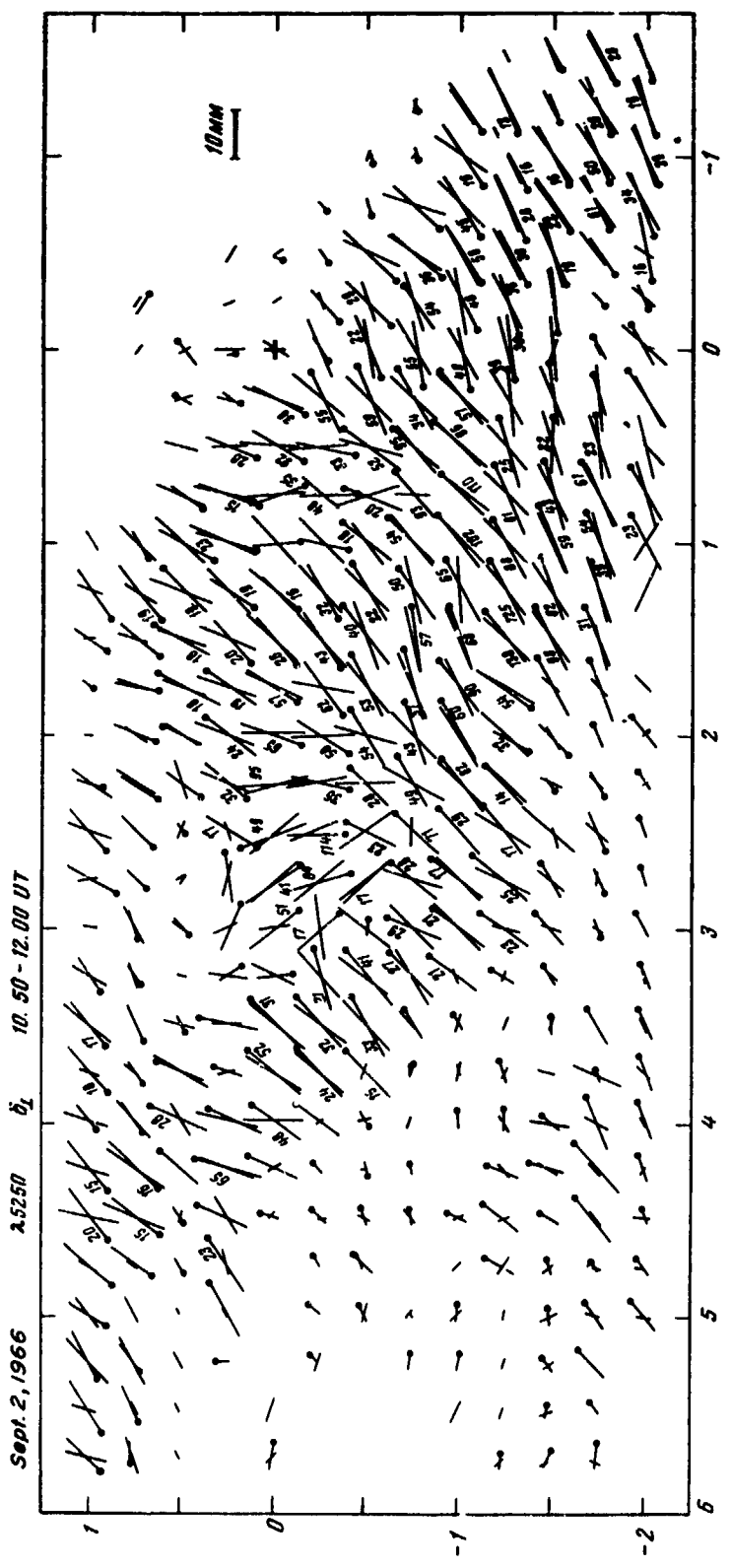


Figure 3. Comparison of Vectors of Transversal Oscillations of  $\delta_L$  Simultaneously Measured on Two Channels but at the One and Same Line,  $\lambda 5250$ , on 2 Sept 1966 (simple stroke = green photometer; stroke with dots = red)

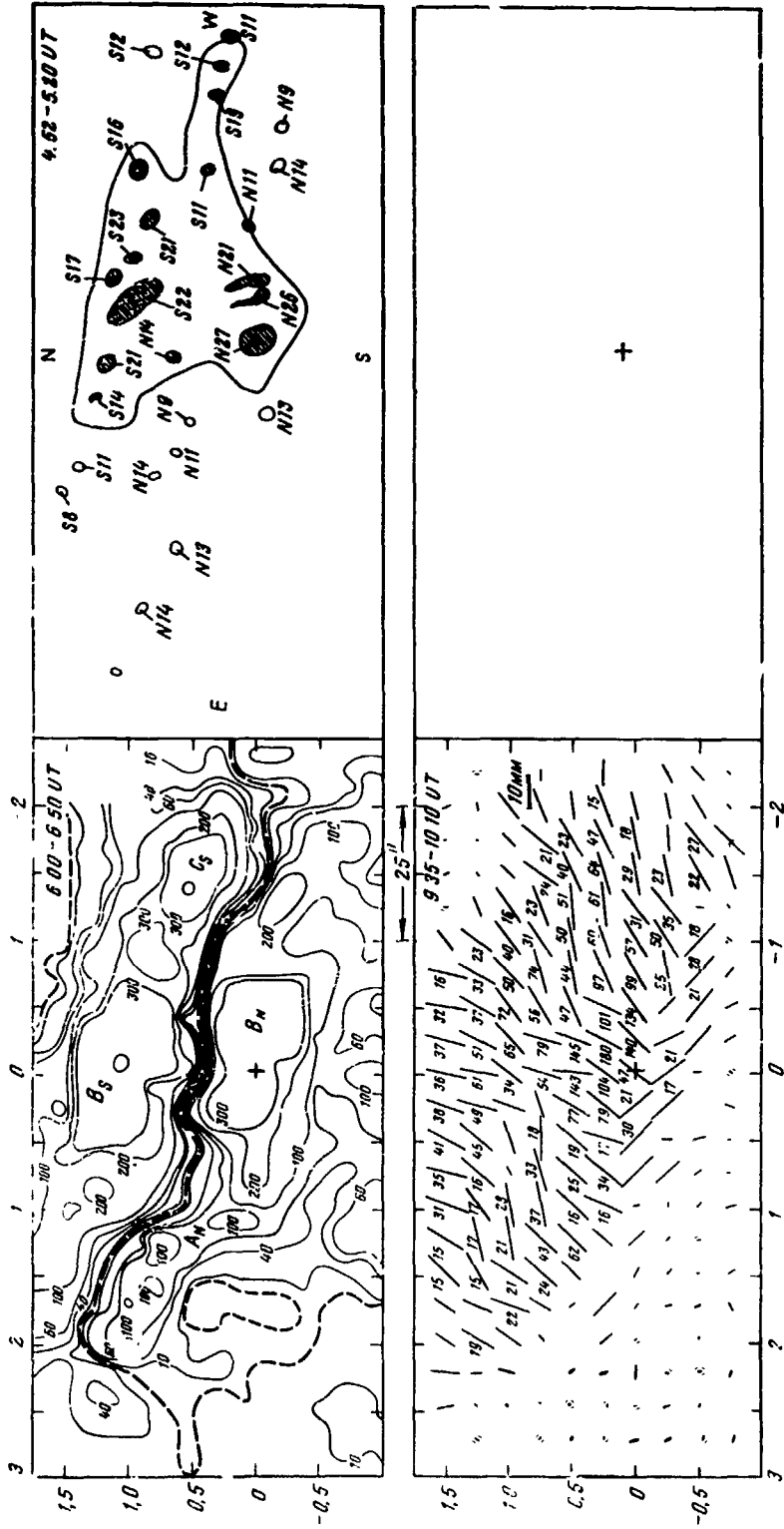


Figure 4. Isogauss Maps of the Longitudinal Field  $H_{||}$  for 5 July 1966 (top left) and of Signals of the Transversal Field  $\delta_{\perp}$  (bottom left). The numbers on the isogauss maps are the values of the transversal field signal in  $gs$ , not corrected for the brightness according to data in Table 1, numbers on the  $\delta_{\perp}$  map are values of  $\delta_{\perp 1} + \delta_{\perp 2}$ , in mm of the original recordings (10 mm scale shown in the right portion of the map). A sketch of solar spots (top right) is made using photoheliogram or drawings obtained from measurements of the spot fields, flare sketch by means of  $H_{\alpha}$ -films. One map can be compared to the other by means of a cross

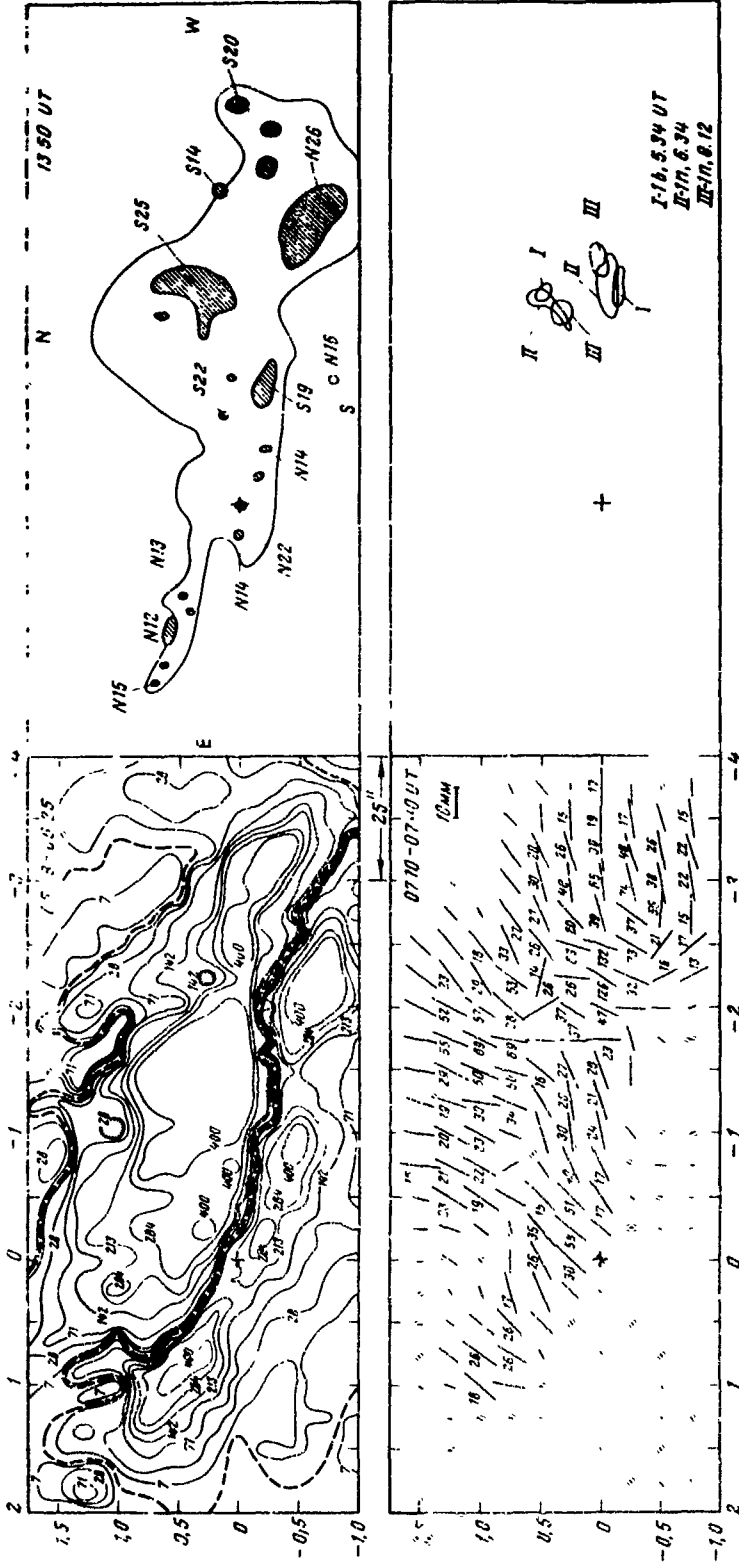


Figure 5. Isogauss Maps of the Longitudinal Field  $H_{||}$  for 6 July 1966 (top left) and of Signals of the Transversal Field 6I (bottom left). The numbers on the isogauss maps are the values of the transversal field signal in gauss, not corrected for the brightness according to data in Table 1, numbers on the 6I map are values of  $\delta 2.1.1 + \delta 2.1.2$ , in mm of the original recordings (10 mm scale shown in the right portion of the map). A sketch of solar spots (top right) is made using photohelioogram or drawings obtained from measurements of the spot fields, flare sketch by means of  $H_{\alpha}$ -films. One map can be compared to the other by means of a cross

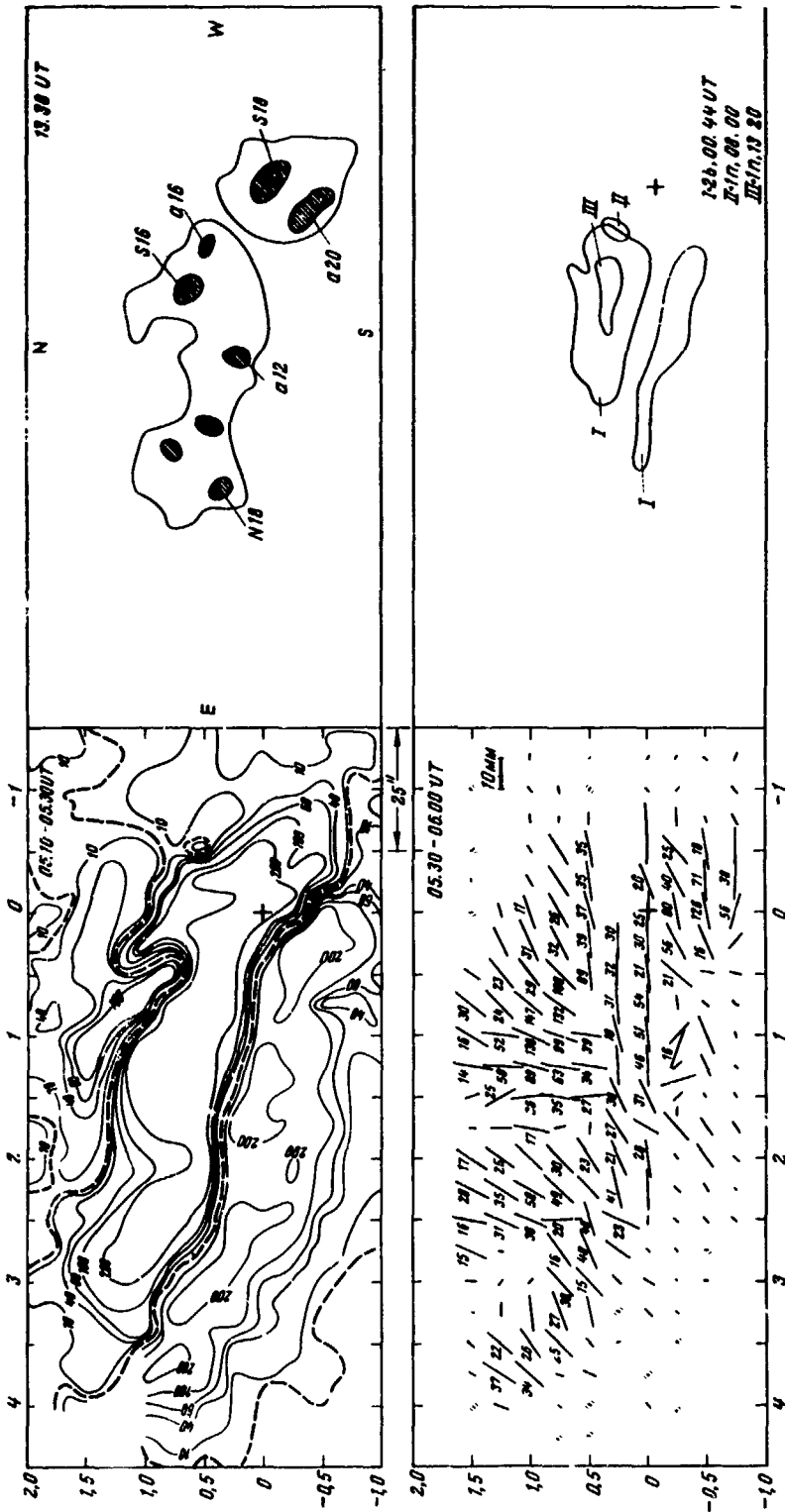


Figure 6. Isogauss Maps of the Longitudinal Field  $H_{\parallel}$  for 7 July 1966 (top left) and of Signals of the Transversal Field  $H_{\perp}$  (bottom left). The numbers on the isogauss maps are the values of the transversal field signal in  $g_s$ , not corrected for the brightness according to data in Table 1, numbers on the  $\delta_{\perp}$  map are values of  $\delta_{\perp 1} + \delta_{\perp 2}$ , in mm of the original recordings (10 mm scale shown in the right portion of the map). A sketch of solar spots (top right) is made using photohellogram or drawings obtained from measurements of the spot fields, flare sketch by means of  $H_q$ -films. One map can be compared to the other by means of a cross

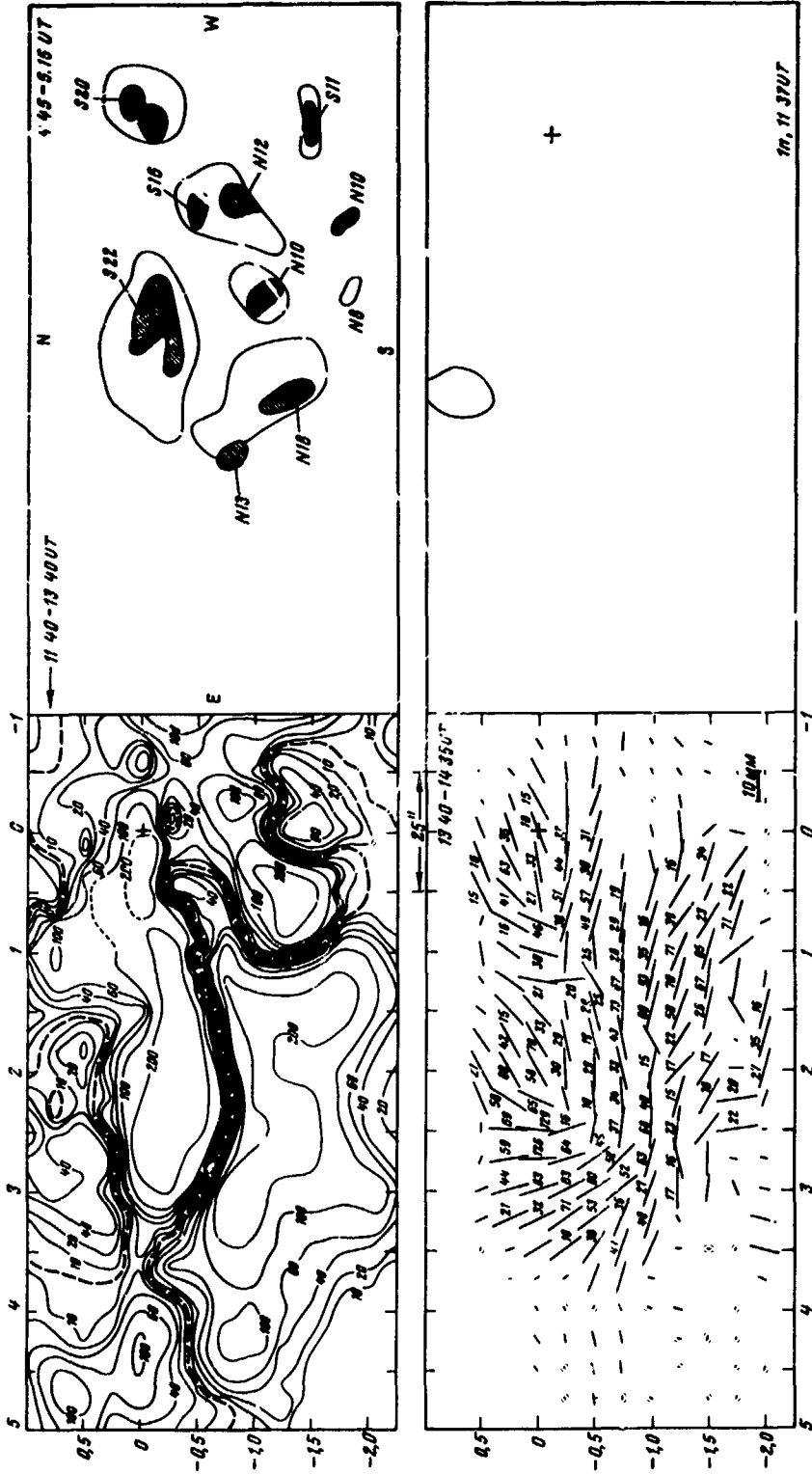


Figure 7. Isogauss Maps of the Longitudinal Field  $H_{||}$  for 30 Aug 1966 (top left) and of Signals of the Transversal Field  $\delta I_{\perp}$  (bottom left). The numbers on the isogauss maps are the values of the transversal field signal in  $gs$ , not corrected for the brightness according to data in Table 1, numbers on the  $\delta I_{\perp}$  map are values of  $\delta I_{\perp 1} + \delta I_{\perp 2}$ , in mm of the original recordings (10 mm scale shown in the right portion of the map). A sketch of solar spots (top right) is made using photohellogram or drawings obtained from measurements of the spot fields, flare sketch by means of  $H_{\alpha}$ -films. One map can be compared to the other by means of a cross



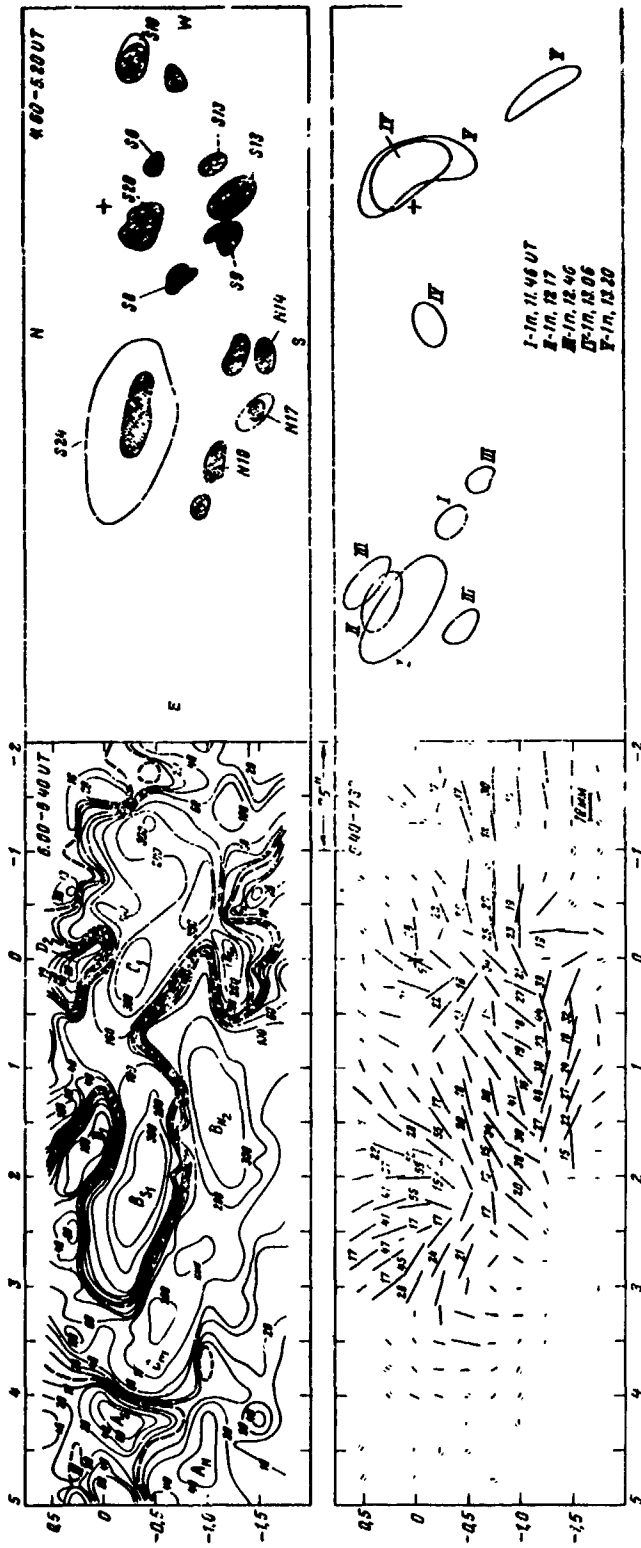


Figure 9. Isogauss Maps of the Longitudinal Field  $H_{\parallel}$  for 1 Sept 1966 (top left) and of Signals of the Transversal Field  $H_{\perp}$  (bottom left). The numbers on the isogauss maps are the values of the transversal field signal in gs, not corrected for the brightness according to data in Table 1, numbers on the  $\delta_1$  map are values of  $\delta_{1.1} + \delta_{1.2}$ , in mm of the original recordings (10 mm scale shown in the right portion of the map). A sketch of solar spots (top right) is made using photohellogram or drawings obtained from measurements of the spot fields, flare sketch by means of  $H_{\alpha}$ -films. One map can be compared to the other by means of a cross

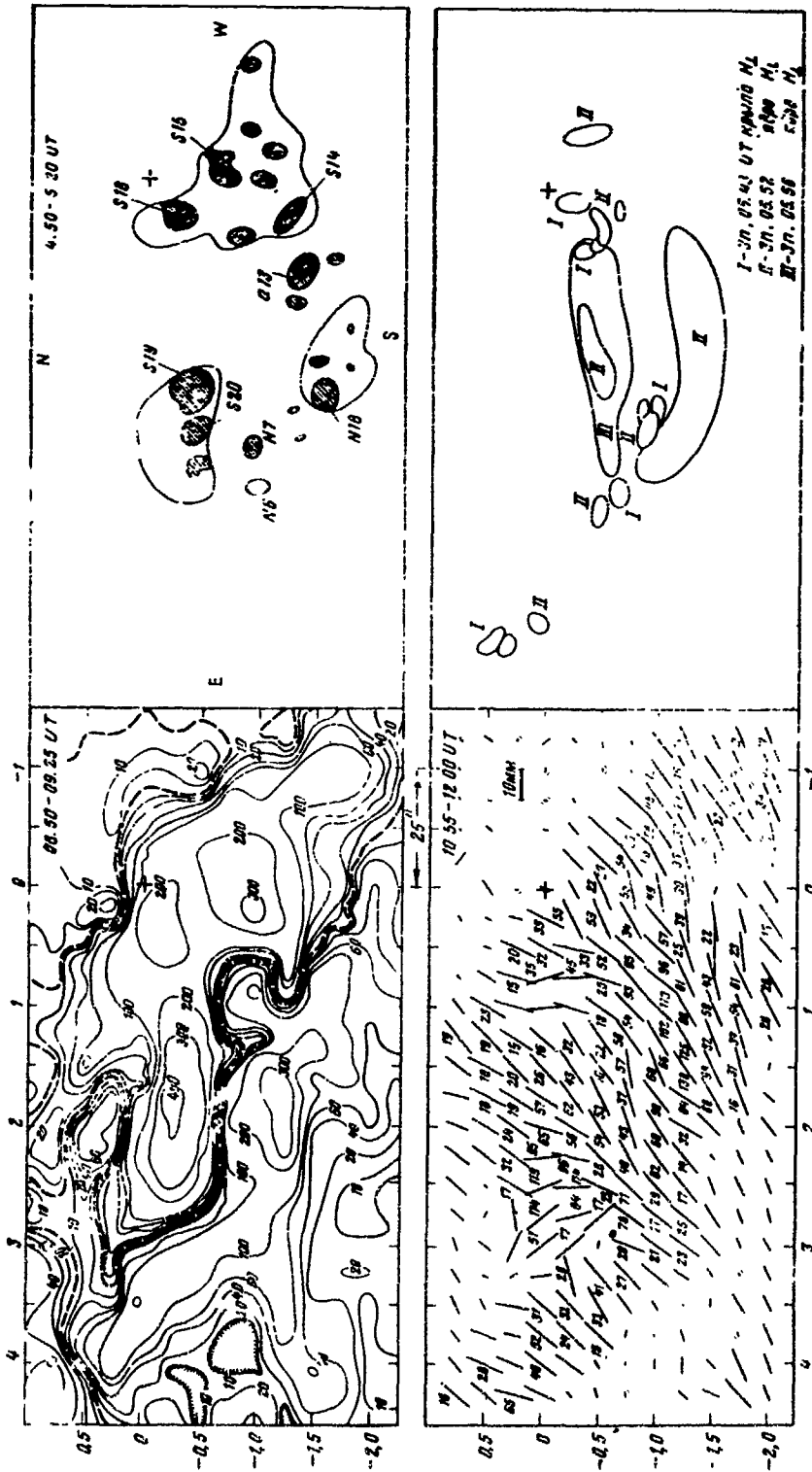


Figure 10. Isogauss Maps of the Longitudinal Field  $H_{||}$  for 2 Sept. 1966 (top left) and of Signals of the Transversal Field  $H_{\perp}$  (bottom left). The numbers on the isogauss maps are the values of the transversal field signal in gs, not corrected for the brightness according to data in Table 1, numbers on the  $\delta I_1$  map are values of  $\delta I_1$  +  $\delta I_2$ , in mm of the original recordings (10 mm scale shown in the right portion of the map). A sketch of solar spots (top right) is made using photohellogram or drawings obtained from measurements of the spot fields, flare sketch by means of  $H_{\perp}$ -films. One map can be compared to the other by means of a cross

considered active region. Recordings of radial velocities were carried out simultaneously (during the recording of  $H_{\parallel}$ ) and of the strength at the center of the lines. In a series of cases (see Table 1),  $H_{\parallel}$  and  $H_{\perp}$  were recorded simultaneously by the method described by Bruns et al., (1964). Field recordings for the first active regions (July 1966) were corrected automatically for brightness oscillations (Nikulin, 1964); during the recording of the second region (Aug - Sept) the automatic installation did not work.

For the calibration of the deflection of the self-recorder of  $H_{\parallel}$  (in  $gs$ ), the following relationships were used (Severnyi, 1964b) for the total deflection of the self-recorder during calibration and passage from the E to W edge of the Sun's image, if recordings of the longitudinal field are carried out separately from recordings of the transversal field  $H_{\perp}$  and the recording is automatically corrected for brightness variation:

$\lambda \text{ \AA}$	5250	6103	4808
E-W ( $gs$ )	1600	2088	3936 .

For simultaneous recordings of  $H_{\parallel}$  and  $H_{\perp}$ , the sensitivity of  $H_{\parallel}$  recordings which theoretically decreased by a factor of two, decreased by a factor of three (according to empirical data). In the case when the brightness compensator was removed (recordings during Aug and Sept 1966), the calibration was performed using the expressions

$$(E-W) (gs) = \begin{cases} 240 I_c / I_o & \text{for } \lambda 5250 , \\ 310 I_c / I_o & \text{for } \lambda 6103 , \\ 588 I_c / I_o & \text{for } \lambda 4808 , \end{cases}$$

where  $I_c / I_o$  is the ratio of the brightness at the center of the disk to the brightness of that region in which the field was measured. Figures 7 to 10 give the isogauss, uncorrected for the brightness of the umbra and penumbra of the spots; this correction was made later during the calculation of gradients, fluxes, and magnetic energy of the field.

Furthermore, the magnetograph signal  $\delta_{\parallel}$  during recordings of  $H_{\parallel}$  is proportional to the actual value of  $H_{\parallel}$  only for small values of  $H_{\parallel}$  ( $\lesssim 100$   $gs$ ); for values of  $H_{\parallel} \approx 300$   $gs$ , the signal  $\delta_{\parallel}$  is practically fully saturated. In order to obtain exact values of  $H_{\parallel}$  in  $gs$ , one used the empirical calibration curve relating the magnetograph signal  $\delta$  with the actual strength of the field  $H_{\parallel}$  (Severnyi, 1967). An analogous empirical curve was used for the dependence of the signal of the transverse field  $\delta_{\perp} / (E-W)$  on the actual strength of the field  $H_{\perp}$  to obtain correct values of the

transverse field. Basic initial results of the analysis of data are the isogauss maps of the longitudinal field  $H_{\parallel}$  and the maps of the distribution of signals of the transverse field

$$\delta_{\perp} = \sqrt{\delta_{\perp 1}^2 + \delta_{\perp 2}^2}$$

(in mm) in the form of dashes, the length of which divided by E-W (Table 1) gives  $H_{\perp}$  (in gs) using calibration curves (Severnyi, 1967). The direction of  $H_{\perp}$  is determined by the formula  $\text{tg } \theta = \delta_{\perp 1} / \delta_{\perp 2}$ .

Figures 4 to 6 give, as most characteristic examples, the maps for 5, 6, and 7 July 1966 for the region which gave a proton flare on 7 July 1966. Figures 7 to 10 show certain selected maps for the second region, which gave two proton flares on 28 Aug and 2 Sept 1966. Sketches are also given there of a group of spots from sketches (or photoheliograms) made during routine measurements of the spots magnetic fields with indication of the field strength (for 6 July 1966 the mean values were taken from data of other observations). Sketches of flares are also given, which were obtained by the projection of  $H_{\alpha}$ -ciné film, taken on the coronagraph KG-1 (shooting in the region outside the band  $\pm 0.5 \text{ \AA}$  from the center of  $H_{\alpha}$  made it possible to readily identify spots on their sketch and on the  $H_{\alpha}$ -film); for the flare of 7 July 1966 which occurred at 0h30m UT, the sketches were obtained from the ciné film SibIZMIRAN\*. The magnetic fields and flares of 28 Aug 1966 were not observed because of bad weather. Comparison of maps and sketches can be made by means of a cross, usually coinciding with the spot, selected for the scanning of the picture of the entire active region (see further detail in Sec 4).

The comparison of maps for different days for the first region on July 5 to 7, show that they are very similar. The same is also true for the second region. Furthermore, the overall similarity of the configurations of the field for the first and second regions is surprising, even though they apparently belong to absolutely different groups. Namely, the first groups which gave the flare on July 7 had a latitude  $\phi = 34$  deg, and in the second turn (July 25 to Aug 7), it either disappeared or shifted very much along the latitude and became transformed into a unipolar spot with a latitude  $\phi = 25$  deg. In the third turn (Aug 24 to Sept 2) at the latitude of 22.5 deg, one observed the second active region which gave a flare on Sept 2.

It is known that in many cases the line of separation of polarities is located close to the north-south direction, separating the leader from the tail spot. At the same time in both considered groups, the boundary, which separates both polarities (or the magnetic axis of the group), is located close to the east-west direction.

---

\*Kindly put at our disposal by V.G. Banin.

Furthermore, entirely similar location of the magnetic axis was noted in many groups with proton flares, for example 14 and 16 July 1969, studied in detail by Howard and Severnyi (1963). It is further typical that among the nine cases of strongest flares with cosmic rays, considered earlier by Severnyi (1963), one observes analogous location of the magnetic axis in seven of them. Namely, these are the cases of flares of: 25 July 1946, 16.14 UT (axis strictly E-W); 19 Nov 1949, 10.30 UT (in this case, the magnetic axis is tilted in the N-E direction at an angle of about 45 deg to the N-S direction); 23 Feb 1956, 03.31 UT (the tilt of the axis is also in the NE direction from the E-W direction at an angle of 30 to 40 deg); the above mentioned flare of 16 July 1959, 21.41 UT (axis in the E-W direction); 12 Nov 1960, 13.15 UT and 15 Nov 1960, 02.07 UT (the axis along E-W); finally, the flare of 1 Apr 1960, 09.15 UT (the axis is slightly tilted in the same NE direction from the E-W direction). Similar location of the magnetic axis of the group, with the same inclination further in the NE direction from the E-W direction, can hardly be termed accidental. It is apparently typical for the majority of groups with proton flares even if the spots and fields are weak, as it was in the case for the flares of 28 Sept 1951. At the same time, it is hardly possible to consider this as a sufficient symptom, since cases of occurrence of proton flares of class 3 were observed in groups where the magnetic axis is located in the N-S direction; for example, flares of class 3 on 7 July 1958, 16 and 22 Aug 1958, and possibly, some others. It would be very important to study this question in more detail.

This similarity of magnetic configuration, in the cases that we are studying, is not accompanied by the similarity of spots configurations of both groups. On the contrary, even for each group, strong variations of the shape and location of the spots in the group are noted from day to day. This situation must be taken into account when attempting to reach conclusions as to the structure of the magnetic field from the external aspect of the groups and spots in it. In such relatively complex groups, such conclusions can turn out to be unreliable.

Furthermore, the similarity of the magnetic configurations does not limit itself by identical location of the magnetic axis. In both cases of the first and second regions, we have two fronts of the magnetic hills of opposite polarities, counter-vailing each other: in the upper region of the S-polarity, it is  $A_S$ ,  $B_S$ ,  $C_S$ , and in the lower it is  $A_N$ ,  $B_N$ ,  $C_N$ ; sometimes two hills merge, and sometimes from three hills a fourth one arises. The analogy is present also in the general character of transverse fields, especially if one compares the first July region with the data of Aug 31 to Sept 2. In both cases, the flux of arrow vectors  $\delta_{\perp}$  in the NW direction (or SE) is clearly noticeable being perpendicular to the direction of the magnetic axis of the group, as can be expected according to simple concepts on the behavior of lines of force between two opposing fronts of the N and S poles.

Conservation of the general similarity of the magnetic configurations with time is accompanied by their even greater analogy at different atmospheric depths, as can be seen from the comparison of maps in  $\lambda 5250$  and  $\lambda 6103$  (for the first region, see Figure 11). The shape of the corresponding isogauss is identical on the maps in  $\lambda 5250$  and  $\lambda 6103$  in all cases (Figure 11). Figure 11 shows for example, that isogauss 600 for  $\lambda 5250$  corresponds to isogauss 400 for  $\lambda 6103$ . At the same time, the comparison made for July 7 shows that the contour of the given strength for  $\lambda 4808$  is narrower than for  $\lambda 5250$ . This also follows from the corresponding planimetry. However, the comparison of longitudinal field maps alone does not yet indicate how the field is distributed with depth (that is, at which depth it is concentrated; see Sec. 5 concerning the total vector of the field). At the same

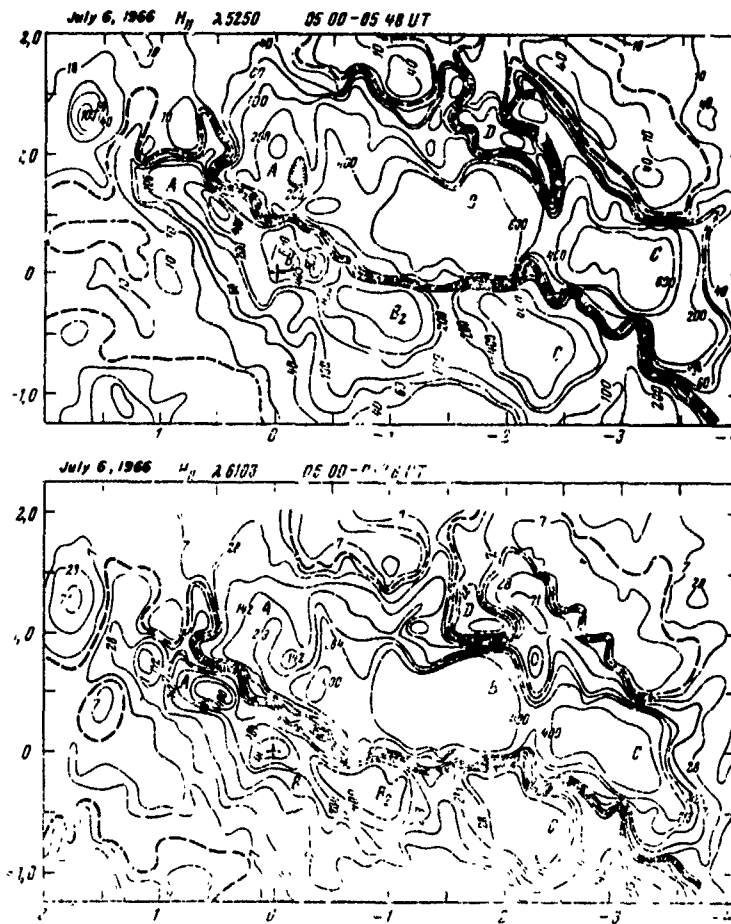


Figure 1 . Comparison of the Isogauss Maps for  $\lambda 5250$  and  $\lambda 6103$  for One Day

time, one can say that the magnetic flux of the longitudinal field decreases in the upper surface layers at least, that is, to the extent that the lines of force diverge as they exit, as could be expected.

The single systematic difference between maps of isogauss  $\lambda 5250$  and  $\lambda 6103$  consists in the presence of a not too large shift of magnetic hills of  $\lambda 6103$  towards the East relative to the hills of  $\lambda 5250$ . This effect is small, about 2.5 arc s on the average for all the hills on the five maps of the first active region for the eastward shift and about 1.8 arc s for the northward shift. For the second region, the data is insufficient. We have one map for 30 Aug 1966, where the average shift is substantially greater and is about 6.7 arc s even though the group of 30 Sept was closer to the center than the group of 4 to 7 July 1966. The variation of the projection effect with the distance from the center must act in the opposite direction, that is, increase the effect to the edge, if the line of force tubes are more or less radial. Consequently, the effect of the shifts is hardly associated with the projection effect.

The best method of verification of the effect was the comparison of maps recorded on two channels in the same line,  $\lambda 5250$ . Comparison for the three cases (30 Aug 1966, recordings at 14.32 to 15.03 and 16.10 to 16.50, and also 2 Sept 1966 at 11.50 to 12.25) also show similar shifts toward the East of 7.0 arc s, 4.4 arc s, and 6.4 arc s, respectively, or an average of 5.9 arc s which is close to the shift along the various lines. Thus, the effect of the shift to the east is most probably due to the instruments, occurring from insufficiently thorough focussing of the picture on the entrance slit of the spectrograph. The small shift sometimes observed in  $\lambda 6103$  towards the north cannot be associated with the phenomenon of atmospheric dispersion, and it is apparently due to the same reason.

In accordance with what has been said in Sec. 1 on the errors of determination of the azimuth of the vector  $\delta_{\perp}$  direction, one can consider that as a rule there is no significant difference between the directions on the maps of  $H_{\perp}$  for both levels ( $\lambda 5250$  and  $\lambda 6103$  as well as  $\lambda 4808$  in the case of the first active region); also the variation of these maps from day to day is insignificant. Only in distinct regions, usually corresponding to the edge of the umbra or penumbra of the spots, can one observe strong rotation during the passage from one line to the other, sometimes reaching 90 deg and perhaps even more. Thus, for example, the comparison of maps for  $\lambda 4808$ ,  $\lambda 5250$ , and  $\lambda 6103$  given in Figure 12a, for 7 July 1966 shows statistically that rotations  $> 30$  deg are encountered in 26% of the cases, when rotations  $\geq 60$  deg are in 8.7% of the cases, which significantly exceeds the possible errors according to data given at the end of Sec. 1. This again justifies the reality of the effect of the strong vector  $H_{\perp}$  rotation during the passage from one line to the other in separate, specific locations of the active regions; in the given case, the directions of the vectors differ little for the lower and middle levels ( $\lambda 4808$  and  $\lambda 5250$ ), and strong rotation is observed for the upper level ( $\lambda 6103$ ).

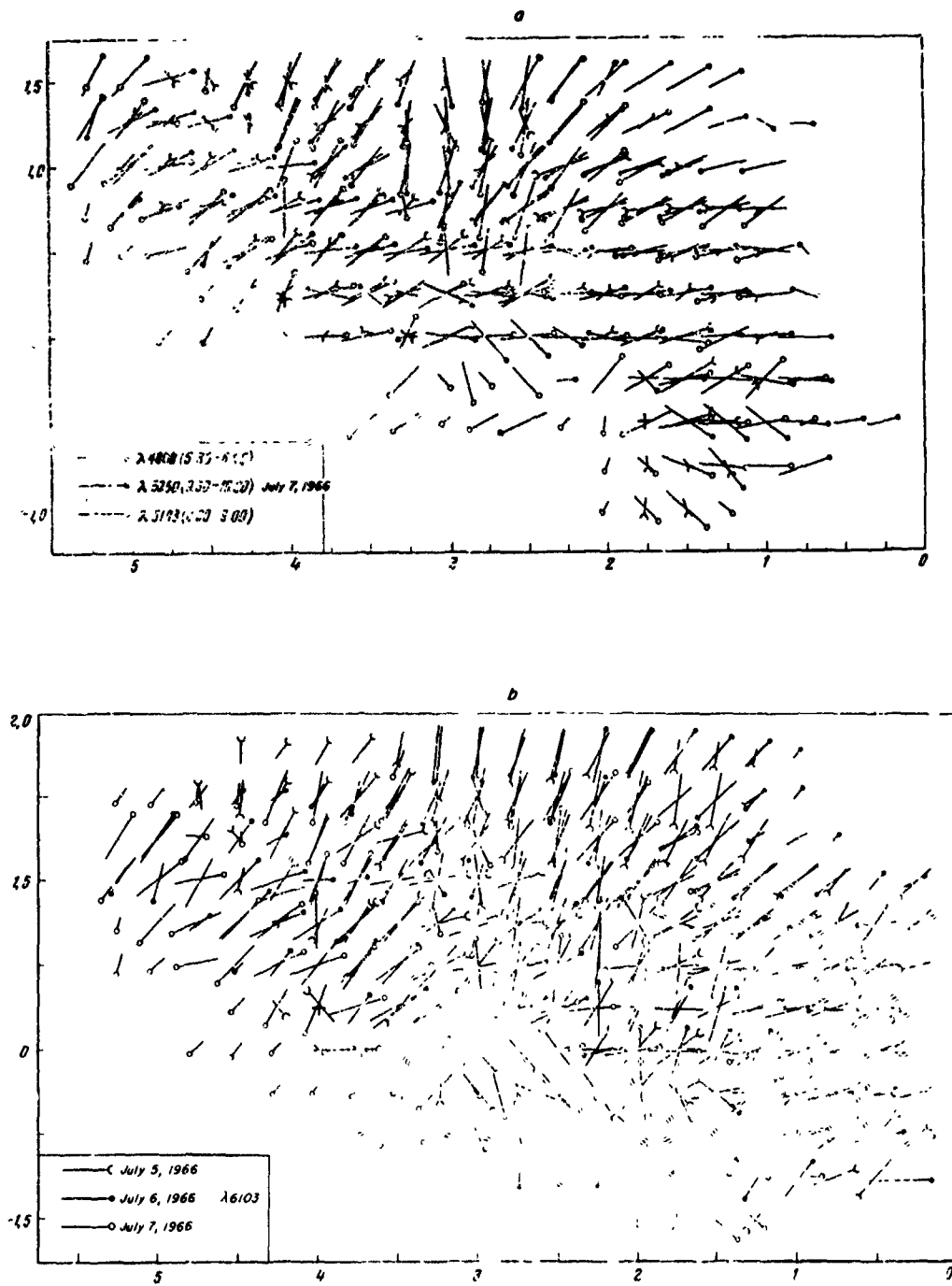


Figure 12. (a) Comparison of the Directions of the Transverse Fields  $H_{\perp}$  for the Same Day on 7 July 1966 in Different Lines; (b) Comparison of Directions of  $H_{\perp}$  for the Same Line on Different Days (July 5, 6, and 7)

Figure 12b shows in general a good agreement between the directions on the map of July 6 ( $\lambda 6103$ ) with the maps for the same level for July 5 and 7. Noticeable difference in the directions of the transverse field occurs for the first time in the middle of the maps, obtained after the proton flare of July 7. If the direction before the proton flare form, roughly speaking, somewhat of a cross in the middle of the map, then after the proton flare there are no signs of vertical intersection, in particular in the region along the vertical from  $y = -0.25$  to  $y = +0.25$ ; instead of vertical vectors  $\delta_{\perp}$ , we have here a flux of practically horizontal directions oriented along E-W, as if the proton flare forced the  $H_{\perp}$  field to orient itself along its extended filaments (compare with Figure 18 which shows the location of the flare relative to the magnetic field). We thus have a rotation by about 90 deg of the vector field at the center of the region during the passage of the map of July 6 to that of July 7 — an effect apparently connected with the proton flare. Analogous effect of the rotation of the vector  $H_{\perp}$  was observed earlier by Severnyi (1964b).

### 3. VARIATION OF THE LONGITUDINAL AND TRANSVERSAL FIELDS (GRADIENTS, FLUXES, FIELD ENERGY)

#### 3.1 Behavior of the Longitudinal Field Gradients

For both proton regions, the distribution of the field strength  $H_{\parallel}$  along the straight line connecting the magnetic hills of opposite signs and same sign polarities  $A_S, B_S, C_S, A_N, B_N, C_N$ , and  $D_N$  was studied (see notations in Figures 2 and 9). The study has immediately shown that if variations with time exist, they are most clearly expressed in the neighboring pairs  $A_S - A_N, B_S - B_N$ , and so forth, while the gradients for the mixed combinations,  $A_S - B_N$ , etc. and hills of the same sign,  $A_S - B_S$ , etc. do not usually show any variation. For closely located pairs, we find certain systematic variations, well defined for the first region and less defined for the second. On Figure 13, examples are given of distributions from which one can find the average gradient  $\Delta H_{\parallel} / \Delta S$ , characteristic for the given direction. For the first region, we have an increase of these gradients  $\Delta H_{\parallel} / \Delta S$  from the initial values (for July 4<sup>d</sup>.4)  $\sim 0.1$  gs/km, long before the flare.  $\Delta H_{\parallel} / \Delta S$  reaches a peak value  $\sim 1$  gs/km for July 6<sup>d</sup>.2 and, after the flare of July 7 (0.30 UT), the values of 0.2 to 0.1 gs/km are reached as well as the initial one (July 7<sup>d</sup>.2). Analogous behavior of  $\Delta H_{\parallel} / \Delta S$  is obtained from the maps for higher levels of the atmosphere  $\lambda 6103$ , even though the variations here are smoother for the same directions than in the case of  $\lambda 5250$ , and the gradients themselves,  $\Delta H_{\parallel} / \Delta S$ , are approximately two times smaller. The results are given in Figure 14.

For the second active region, the gradients themselves are 2 to 3 times smaller than for the first. The variations of the value of  $\Delta H_{\parallel} / \Delta S$  are well expressed only

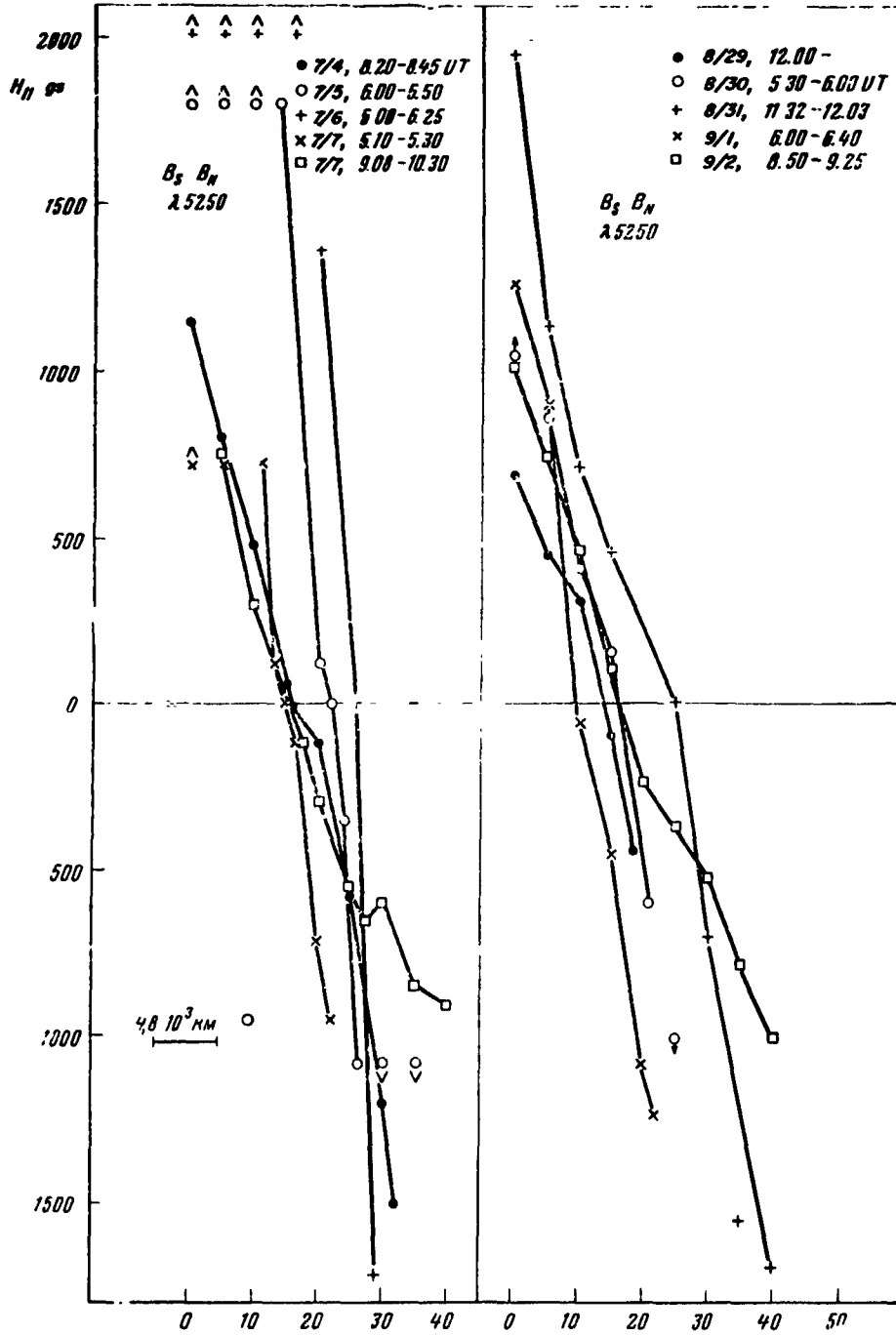


Figure 13. Distribution of the Strength of the Longitudinal Field  $H_{||}$  Along the Straight Line Connecting Hills of Different Polarities for Various Days for the First (left) and Second (right) Active Regions

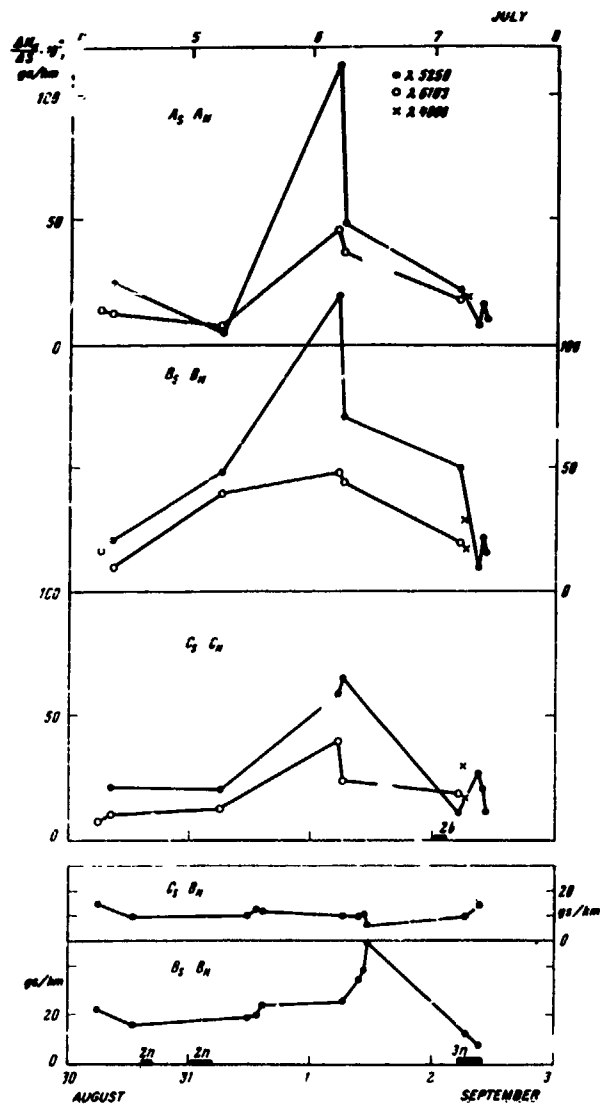


Figure 14. Behavior of the Average Gradients of the Field  $\Delta H_{||} / \Delta S$  with Time for Certain Characteristic Directions for the First (top) and Second (bottom) Active Regions

and also with two flares of importance 2n on Aug 30. Unfortunately, there are no variations of the magnetic field close to the flare of Aug 28. At the same time on Sept 1, an increase in the gradient  $\Delta H_{||} / \Delta S$  was clearly noticeable up to the values of about 0.5 gs/km which, after the flare of 2 Sept 1966 (measurements were made shortly after the event), returns to the initial low value, slightly below 0.1 gs/km.

for one direction,  $B_S B_N$ , (for comparison the behavior of this value for the direction  $C_S B_N$  is also given). The amplitude of the oscillations of  $\Delta H_{||} / \Delta S$  is 2 to 3 times smaller (hills  $A_S$  and  $A_N$  disappeared during further development of the region). The values of  $\Delta H_{||}$  given in Figure 14 are corrected using a calibration curve (Severnyi, 1967), and in addition, for the second active region, correction of the field strength was made for the brightness at all points where selected directions intersected the umbra or penumbra of the spots. Simultaneous recording of the strength show that for the penumbra, the value of the strength of  $H_{||}$  must be increased on the average by 1.4 times, and by approximately two times in the umbra region. It is possible that the most "sluggish" variations and increase of  $\Delta H_{||} / \Delta S$  prior to the Sept 2 flare are connected with the appearance of a strong flare directly prior to the considered period, namely a flare of importance 3n on Aug 28,

### 3.2 Behavior of the Field Fluxes

The behavior, similar to that of  $\Delta H_{\parallel} / \Delta S$  is shown by the sum of the fluxes of both polarities  $F_S + F_N$  obtained by means of planimetry of the isogauss  $H_{\parallel}$  maps (Figure 15). For the July group, this value increases up to the peak values ( $27 \times 10^{21} \mu\text{cp}^*$  for  $\lambda 5250$  and  $25 \times 10^{21} \mu\text{cp}$  for  $\lambda 6103$ ), and then after the flare of July 7, the initial conditions are re-established. The relative increase of the field in a deeper layer ( $\lambda 5250$ ) is practically the same as in the outer layer ( $\lambda 6103$ ).

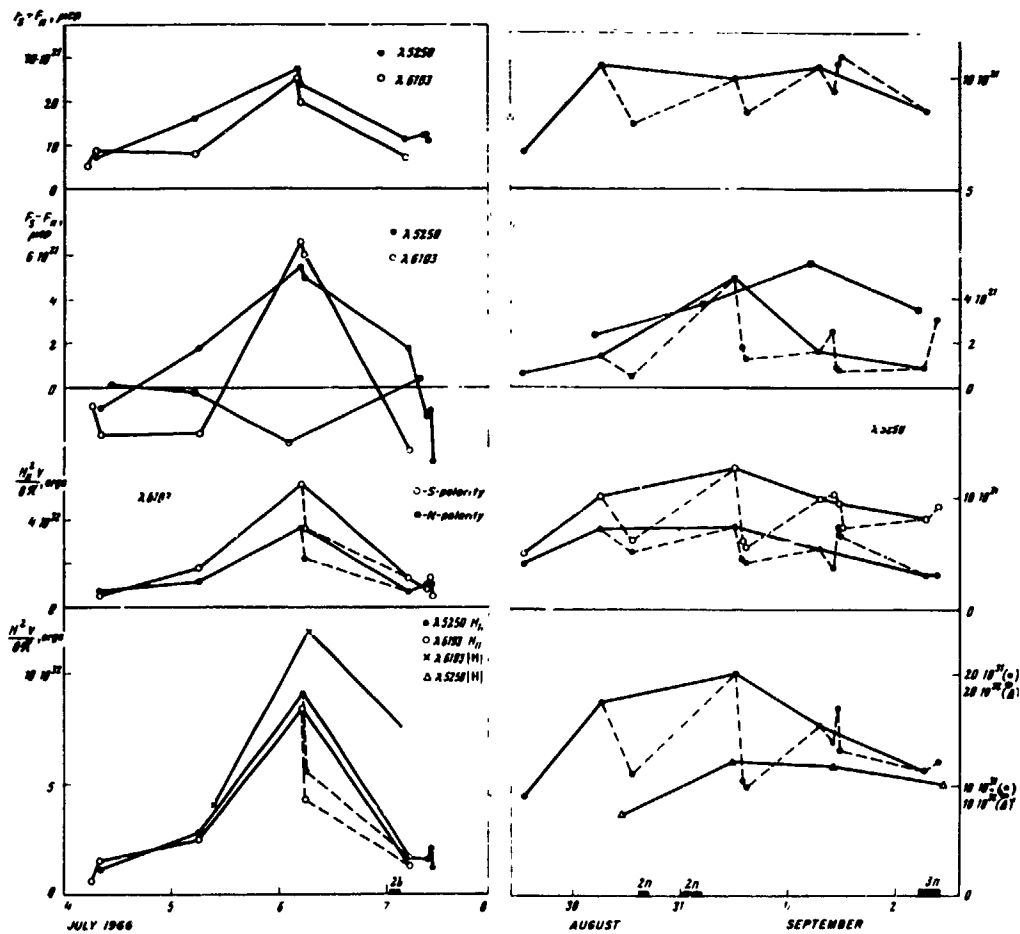


Figure 15. Variations of the Magnetic Energy of the Absolute Field  $|H|^2 V / 8 \pi$  and of the Longitudinal Field  $H_{\parallel}^2 V / 8 \pi$  with Time. Behavior of the total flux  $F_S + F_N$  and "imbalance" of the fluxes  $F_S - F_N$  with time for the first and second active regions. Circles with dots are the value of  $F_S - F_N$  from sketches of the spots by Solar Services

\*Editor's Note: The unit of magnetic flux, one maxwell, has erroneously been translated to  $\mu\text{cp}$  throughout the text. Read mx for  $\mu\text{cp}$ .

The "imbalance" of fluxes  $F_S - F_N$  (S-polarity of the leading spot) behaves in the same manner. However the initial and final values here are negative and comprise about 0.1 of the peak value ( $\sim 10^{22} \mu\text{cp}$ ). In our case, there is a relative increase of the flux of S-polarity as compared to that with N-polarity prior to the flare. These results are in general agreement with the results of Martres et al. (1968a) for the nine flares of the QSAR period. Namely, these authors have obtained the decrease of the total flux  $F_S + F_N$  in the sense that before the flare, the flux is greater than after it (from nine flares, with a decrease in one case). Prior to the flare, according to Martres et al. (1968a), the imbalance (that is, the flux of the leader minus the flux of the tail spot) is greater than after it. There is a tendency of increase of probability of occurrence of flares with the increase of the difference  $F_S - F_N$ . In our case of the proton flare, it is difficult to speak of the leader, since the x-axis of the group is located almost in the E-W direction, but leading in the new cycle are the S-polarity in the N-hemisphere. Therefore, the meaning of difference is the same as in the work of Martres et al. (1968a).

For the second group (see Figure 15, right), the value  $F_S - F_N$  is two to four times smaller, and the variations are not as strongly expressed as for the first group. Here, furthermore, because of poorer resolution in the middle of the day, a drop of field strength and fluxes from morning to midday and further, is noted. This is a systematic effect analogous to the one found by H. Kunzel (1967) which sometimes is erroneously interpreted as the effect of real field variations. Actually, from recordings of field  $H_{\parallel}$  strength simultaneously with photoelectric recordings of the contrast, one of the authors recently discovered that the majority (not less than 80%) of such variations – a drop of the field down to 30% – is connected with the picture contrast decrease. One must therefore base oneself on the morning, with best measurement of the picture quality, which are connected by a continuous line in Figure 15. (Apparently the drops of the field, because of the worsening of contrast, are the most strongly reflected on the value of the field energy, see below.) The general behavior of the values of  $F_S + F_N$  and  $F_S - F_N$  for the second group also indicate an increase in the imbalance of  $F_S - F_N$  and certain increase of the flux approximately a day before the flare, although here this effect is not as clear as in the July group.

The behavior of the magnetic energy of the longitudinal field

$$\sum \frac{H_{\parallel}^2}{8\pi} V_i$$

can also be clarified by means of planimetry of the isogauss maps, by multiplying the strength  $H_i$  of the isogauss by the areas, enclosed between the  $i$  and  $i + 1$  isogausses, and by the "depth", which we take equal to  $10^4$  km. For the July 1 group,

the energy  $\Sigma H_{\parallel}^2 V_i / 8\pi$  increases from 1 to  $2 \times 10^{32}$  to  $9 \times 10^{32}$  ergs during the period from 4<sup>d</sup>.3 to 6<sup>d</sup>.2, and then after, the proton flare falls to the initial values. Similar variation of the energy is observed for  $\lambda 6103$ , but the values here are somewhat smaller than for the lower ( $\lambda 5250$ ) level. In both cases, the variations are clearly and well defined, and the very existence of these variations is fully reliable, since it appears independently along two lines and is ascertained as a rule by two measurements a day. Resolution during the period of observations was satisfactory even though here also one can observe a tendency of the field drop towards the middle of the day (well noticeable for July 6 on the graphs of energy of S and N polarities, taken separately). The excess of the energy of the leading S-polarity which at the beginning (July 4) was absent and reached the greatest value before the flare (July 6) and dropped again after the flare, is well noticeable.

For the Sept 2 flare, the picture is similar, even though the energy maximum is attained approximately a day prior to the flare. The energy of the S-polarity also exceeds, by almost a factor of two, the energy of the N-polarity, and this excess remains during the flare. There is an impression created that the Sept 2 flare occurred "at the tail" of these variations of the fields which were observed in this group. The energy of this group was four to five times smaller than the energy of the July group, and the relative energy increase for the Sept 2 group is two times smaller, from a minimum value of about  $9 \times 10^{31}$  ergs to a maximum of about  $20 \times 10^{31}$ , and then a drop to  $11 \times 10^{31}$ , which is significantly smaller (by approximately ten times) than that increase observed for the July group. It is possible that all the effects of Sept 2 were connected with this and were significantly smaller than the one observed for the flare of July 7. One must, finally, note that not only the magnetic configurations of both studied groups are very similar with the configuration of the group which gave the greatest proton flare of 16 July 1959, but that the behavior of the gradient  $\Delta H_{\parallel} / \Delta S$  and the energy  $H_{\parallel}^2 V / 8\pi$  is very similar to the one observed for this flare, as described by Howard and Severnyi (1963).

Although the total strength of the field (longitudinal and transversal) will be studied in Sec. 5, one should note now the behavior of the values of the absolute energy on the same Figure 15 calculated by planimetry of the isogauss maps of the absolute strength  $|H|^2 V / 8\pi$ . This behavior in general is similar to the behavior of the energy of the longitudinal field. Therefore, one cannot fully relate the variation of the energy of the longitudinal field to the redistribution of energy among the components  $H_{\parallel}$  and  $H_{\perp}$  with time. That is, consider that before the flare, there is an increase of the "longitudinal" energy because of the "transversal" energy, and vice versa. In other words, consider the variations of the configurations, such that, when the field prior to the flare is more longitudinal, afterwards it is more transversal. However, to some extent, this can be justified for the flare

of July 7, since the energy of the absolute field decreases not as much (by about two times) as the energy of the longitudinal field (a decrease by about four times). To a greater degree, this is justified for the Sept 2 flare where the variation by 1.2 times of the total energy is accompanied by the decrease of the energy of the longitudinal field by about 1.8 times. It is possible that this very flare or the processes accompanying it (eruption discharges) and in particular preceding it, lead to a more "longitudinal" configuration of the field, elongated in the radial direction away from the sun.

In all the above considered variations of the energy and fluxes associated with proton flares as well as in the case of the proton flare of 16 July 1959, there are no indications as to when they occur, since we did not have measurements directly before the flares. Only for the case of a strong flare of importance 2, on 22 June 1962, do we possess measurements of the  $H_{\parallel}$  and  $H_{\perp}$  fields directly before, during, and after the flare. Maps of the field, given by Severnyi (1964b) were subjected to planimetry and fluxes and the energy were calculated by the same method as before. Figure 15 gives results witnessing that the flare is more a result of a preliminary

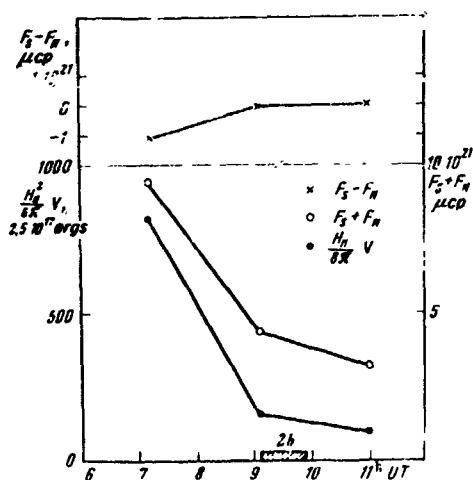


Figure 16. Behavior of the Magnetic Energy of the Longitudinal Field  $H_{\parallel}^2/8\pi$  of the Total Flux  $F_S + F_N$  and the Resulting Flux  $F_S - F_N$  with Time for the 22 June 1962 Flare

drop of strength and energy of the field rather than a phenomenon which accompanies or precedes it. This example is so far unique, and the collection of a greater amount of data is needed for reaching more certain conclusions on the timely sequence and relationship of events.

Some features of the variations described in this section require a more careful examination. First there is a variation of the "imbalance" of fluxes or the resulting magnetic field  $\Phi = F_S - F_N$  with time. For the first active region, this flux was varying before the flare of July 7 from the value of  $-2 \times 10^{21} \mu\text{cp}$  to  $+7 \times 10^{21}$ , that is, by  $9 \times 10^{21} \mu\text{cp}$  per day (from 5<sup>d</sup>26 to 6<sup>d</sup>22). Analogous variation before the Sept 9 flare

comprised approximately  $4 \times 10^{21} \mu\text{cp}$  during the period from 29<sup>d</sup>52 to 31<sup>d</sup>48, that is, approximately over the period of two days or  $3.5 \times 10^{21} \mu\text{cp}$  from 30<sup>d</sup>24 to 31<sup>d</sup>48, that is 1<sup>d</sup>24. This gives the flux variation\*

\*It is assumed that the values of  $\Delta\Phi/\Delta t$  before the flare are minimum (average). Actual values can be substantially greater.

$$\frac{\Delta\Phi}{\Delta t} = \begin{cases} \frac{c \times 10^{21}}{8.6 \times 10^4 \times 0.96} = 1.09 \times 10^{17} \mu\text{cp/sec (for the first region)} \\ \frac{3.5 \times 10^{21}}{8.6 \times 10^4 \times 1.24} = 0.33 \times 10^{17} \mu\text{cp/sec (for the second region).} \end{cases} \quad (1)$$

It was of interest to verify this and to investigate the behavior of the fluxes  $F_S + F_N$  and  $F_S - F_N$  for a previously studied (Howard and Severnyi, 1963) powerful flare with cosmic rays on 16 July 1959. Figure 17 gives the behavior of these

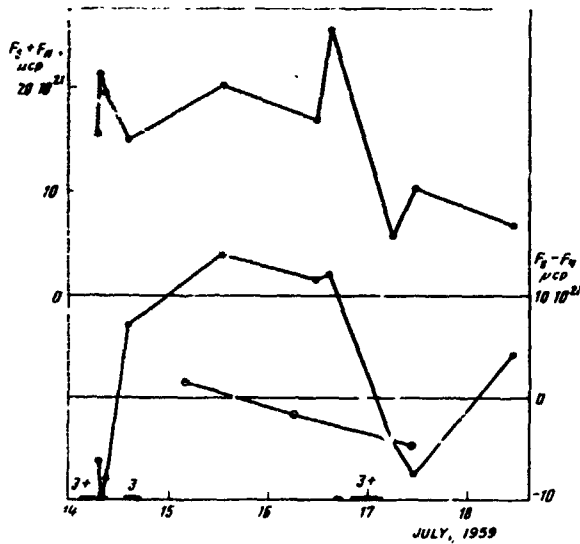


Figure 17. Behavior of the Total Flux  $F_S + F_N$  and Resulting Flux  $F_S - F_N$  for the 16 July 1959 Flare (dots). Circles with dots have same values from the sketches of solar spots by Solar Services

fluxes from 14 to 18 July 1959 from planimetry data of isogauss maps given by Howard and Severnyi (1963). We see here the same picture

as for the investigated proton flares: the increase of the  $F_S + F_N$  flux directly before the flare (possibly during the flare) and also very strong and with the same sign, and the imbalance of  $F_S - F_N$  before the flare. One cannot but associate the sharp decrease of the resulting flux of  $F_S - F_N$  from the value of  $+12 \times 10^{21} \mu\text{cp}$  to  $-8 \times 10^{21} \mu\text{cp}$  during the period from 16<sup>d</sup>62 to 17<sup>d</sup>46, that is, during 0<sup>d</sup>84 =  $7.25 \times 10^4$  sec, with the flare of July 16, which gives

$$\frac{\Delta\Phi}{\Delta t} = 2.75 \times 10^{17} \mu\text{cp/sec.}$$

Somewhat lower values of  $\Delta\Phi/\Delta t$  follow from Martres et al. (1968a), where one basically considered regular non-proton flares. From the table of values of  $\Phi$ , given both in the works of Martres et al. (1968a) and from the maps of isogauss of the Crimean Astrophysical Observatory for instants directly before the flare and after it, one obtains the following values  $\Delta\Phi/\Delta t$  (see Table 2.  $\Delta t$  varies between 2 and 6<sup>h</sup>).

Apparently, for the sake of orientation one can consider that for small flares, the typical value of  $\Delta\Phi/\Delta t \approx 0.1$  to  $0.2 \times 10^{17}$ , when for strong flares, it is of  $-1.0 \times 10^{17} \mu\text{cp}/\text{sec}$ . Since  $1\text{v} = 10^8 \text{CGSM} = 1/300 \text{CGSE}$ , then according to Maxwell's equation, the emf (in volts) induced during the variation of the flux  $\Delta\Phi/\Delta t$  is

$$\oint \text{Eds} = -10^{-8} \Delta\Phi/\Delta t. \quad (2)$$

If  $\Delta\Phi/\Delta t$  is expressed in  $\mu\text{cp}/\text{sec}$  (in CGSM units), then

$$\oint \text{Eds} = \begin{cases} 1/2 \times 10^8 \text{ v (weak flares)} \\ 1.0 \times 10^9 \text{ v (strong flares)}. \end{cases} \quad (3)$$

Table 2

Date	Flare UT	Class	$\Delta\Phi/\Delta t$ $\mu\text{cp}/\text{sec}$	Date	Flare UT	Class	$\Delta\Phi/\Delta t$ $\mu\text{cp}/\text{sec}$
18 Aug 1959	10.19	3	$-0.83 \times 10^{17}$	4 Oct 1965	9.37	2	$-0.16 \times 10^{17}$
19 Mar 1965	9.40	1	$-0.65 \times 10^{17}$	23 Aug 1958	17.17	1+	$-0.16 \times 10^{17}$
5 Sept 1965	8.12	1-	$+0.57 \times 10^{17}$	22 June 1962*	9.06	2	$+1.31 \times 10^{17}$
	9.40	1-					
30 Sept 1965	13.13	1	$-1.28 \times 10^{17}$	7 June 1966*	0.26	2+	$+1.09 \times 10^{17}$
1 Oct 1965	11.40	1	$+0.12 \times 10^{17}$	2 Sept 1966*	5.44	2+	$+0.33 \times 10^{17}$
2 Oct 1965	10.45	1-	$+0.22 \times 10^{17}$				
	12.34	1-					

These values agree so well with the proton energies (100 to 1000 Mev), which are generated during the flares\* that the question arises whether the emf lies in the basis of this generation in the contour comprising the active region in the limits of which occur the actually measured variation of the magnetic induction flux. One should note that the value of the flux  $\Phi$  always (each and every time) is measured

\*The force  $W$  for a potential difference  $V_1 - V_2$  (v):  $W = \frac{e(V_1 - V_2)}{300}$ , where  $e = 4.80 \times 10^{-10} \text{CGSE}$  - electron charge, that is,  $W = \frac{480}{3} (10^{-4} \text{ to } 10^{-3} \text{ ergs})$  or  $W = 10^7 \text{ to } 10^9 \text{ ev}$ , that is, 100 to 1000 Mev ( $1 \text{ ev} = 1.60 \times 10^{-12} \text{ ergs}$ ). Similar remarks are probably unnecessary, since it is a reminder of well known definitions, and it is used only for convenience in comparing energies in various units.

for the one and same (geometrical) region on the map, the boundaries of which ("contour" of integration) is determined by a somewhat arbitrary selection of the "periphery" of the active region. However, this is immaterial, since it is easy to convince oneself (from review, for example, of maps of  $H_{\parallel}$  in Figures 4 through 10 and others, not given), that all variations of the value of  $\Phi$  are related with the variation of the location of isogauss inside this fixed region basically a closed region with S-polarity, in the area of strong ( $\geq 300$  to 500 gs) fields; contribution from the periphery to the variation of  $\Phi$  is insignificantly small and comprises not more than 10 to 20%. Furthermore, it is difficult to compensate the "imbalance"  $\Phi$  (the excess of the S-flux which rapidly occurs before the flare) by the N-flux which is somewhere around the region of low below-the-noise-level fields. Indeed, if this were so, then to compensate the flux around  $10^{22} \mu\text{cp}$  for a field  $H = 1$  gs (noise level), one would need a region with an area of  $10^{11}$  cm<sup>2</sup> — almost 1.5 times the radius of the Sun, which is improbable.

One should also note that one cannot judge the behavior of  $\Phi = F_S - F_N$  imbalance in the groups from the routine data of the Solar Services, that is, from fluxes obtained by multiplying the areas of umbra spots by the corresponding measured peak strength, summarizing these products for N- and S-polarity and then subtracting. This is very well seen on Figures 15 and 17 where the data found by means of Solar Services sketches (or photoheliograms) are given in the graphs of  $F_S - F_N$  as a dot with a circle. We see that for the 2 Sept 1966 flare, one obtains a behavior more or less close to the one which follows from the planimetry of isogauss maps. For the 16 July 1959 flare, these  $F_S - F_N$  data do not show any variation of the flux even though planimetry gives a well-defined effect, and for the 7 July 1966 flare, one even obtains a behavior opposite (in sign and magnitude) to that which follows from planimetry. One cannot rely on the picture of the nuclei of spots and of the strength of their field, not only because they do not always give  $H_{\parallel}$ , but because the main source of errors consists in that the nuclei sometimes contribute very little to the area into the resulting flux, as for example, that which occurred on 5 to 7 July 1966, when the nuclei of the spots of S-polarity of July 5 and 6 remained fine, at the time when nuclei of the N-polarity already grew strong by July 6 (especially the leader). Only the areas of the nuclei of S- and N-polarities of July 7 became more or less equal. At the same time, the area of the S-polarity region was growing much faster, according to the isogausses, before the flare than the same one for the N-polarity, and the S-polarity isogausses, with greater strength, occupied a region much larger than the total area of the S-spots nuclei.

The "imbalance" of fluxes is a phenomenon generally characteristic for groups of spots: essentially a unipolar spot is an extreme example of such an "imbalance". However, while it is stationary, which is usually observed, there is no flux variation. Such "imbalance" is also noted on the stage of development of the bipolar

group (Gopasyuk, 1967a) when one of the spots (leader or tail) grows in such a way that the imbalance of fluxes of both spots existing in the growth stage decreases and disappears at the end of the group development\*. Thus, for example, it was found by Gopasyuk (1967a) that the imbalance  $\Phi = 2 \times 10^{20} \mu\text{cp}$  (that is, the tail region minus the leader region) existing in the initial development phase disappeared after 12 hr. This gives

$$\frac{\Delta\Phi}{\Delta t} = \frac{2 \times 10^{20}}{4.3 \times 10^4} = 4.65 \times 10^{15} \mu\text{cp/sec}$$

which is 10 to 20 times smaller than the values found above for the proton regions. It is possible that this means for usual non "proton" regions, we cannot expect the appearance of substantial emf's and the generation of particles with energies greater than a few Mev for flux variations, that is, such regions cannot be sources of hard particles. Since group decay is also accompanied by flux imbalance, apparently then, one can assume that the emf and the particle generation can be associated with the growth phase or that of decay of the group of spots. To this corresponds a well known fact that the flares appear most frequently during the period of growth and decay of spot groups.

However, the measured variation of the flux relates to the region bound by a stationary geometric contour, for which emf is calculated. Inasmuch as plasma moves, we must know the flux through the area bound by the moving contour is associated with the one and same group of particles. Flux variation through the area of a contour moving with a velocity  $v$  is (see for example, the works of Alfvén and Fälthammar, 1963)

$$\begin{aligned} \left( \frac{d\Phi}{dt} \right)_{\text{Mov.}} &= \iint \frac{\partial H}{\partial t} ds + \oint (v \times ds) H = \left( \frac{\partial \Phi}{\partial t} \right)_{\text{stat}} - \iint \text{rot} (v \times H) ds \\ &= -c \iint \text{rot} \left( E + \frac{1}{c} [v \times H] \right) ds; \end{aligned} \quad (4)$$

according to Maxwell's equation

$$\text{rot } E = - \frac{1}{c} \frac{\partial H}{\partial t}.$$

Otherwise, Eq. (4) can be written as

$$- \frac{1}{c} \left( \frac{\partial \Phi}{\partial t} \right)_{\text{mov}} = \oint E' ds, \quad (5)$$

\*Conservation of the flux balance for a developed group was found by Stenflo (1968) (see Sec. 7).

where  $E'$  is the strength in the moving contour

$$E' = E + \frac{1}{c} [\mathbf{v} \times \mathbf{j}] \cdot \frac{\mathbf{j}}{\sigma}, \quad (6)$$

where  $\mathbf{j}$  is the current density; Eq. (6) also directly follows from the Lorentz transformation (Alfvén and Fälthammer, 1963, para. 1 through 3) for  $\sigma = \infty$ ,  $E' = 0$  and  $(d\Phi/dt)_{\text{MOV}} = 0$ , that is, the flux through the region supported by the moving contour does not change; emf in this contour is equal to zero. Let us, however, evaluate the actual value of  $E'$ . We are measuring the value of emf for a stationary contour

$$-\frac{1}{c} \left( \frac{\partial \Phi}{\partial t} \right)_{\text{stat}} = \oint E_{\text{DS}} = 3.33 (10^5 \text{ to } 10^6) \text{ CGSE}$$

and letting the length of the contour be of the order of the length of the active region  $L = 10^{10}$  cm, we obtain

$$E = \begin{cases} 3.33 \times 10^{-4} & \text{for strong flares} \\ 3.33 \times 10^{-5} & \text{for weak flares.} \end{cases} \quad (7)$$

The emf associated with the motion and the induction intensity  $\frac{1}{c} \mathbf{v} \times \mathbf{H}$  can be estimated by a different method: (a) from the reduction of the region of S-polarity, as it can be judged from the location of the line  $H_{\parallel} = 0$  and individual isogauss on the maps of the longitudinal field in Figures 4 through 10 and others; (b) from the variation (expansion) of the size of the penumbra and the spot nuclei; (c) from the variation of the distances between the one and same spots; and (d) from the direct measurements of longitudinal beam velocity for the groups at the edge of the disk with a magnetograph. The average values of maximum velocities, evaluated in such a manner are given in Table 3.

Table 3

Method	1st Region cm/sec	2nd Region cm/sec	Method	1st Region cm/sec	2nd Region cm/sec
a	$0.85 \times 10^4$	$1.05 \times 10^4$	c	$0.50 \times 10^4$	-
b	penumbra	$0.95 \times 10^4$	d	$\leq 1.50 \times 10^4$	$\leq 1.50 \times 10^4$
	nucleus	$1.20 \times 10^4$			

The obtaining of these values may be clarified by means of an example. Consider a comparison of situations in a group and in magnetic fields on July 6 and 7; (a) maps on Figures 5 and 6 show that the closed region of S-polarity shrunk on July 7 in the N-S direction from 8.5 to 13.5 arc s (from 7 to 11.5 km per day) which gives a velocity  $v_a = (0.9 \text{ to } 1.3) \times 10^4$  cm/sec. From the isogauss  $H_{\parallel} = 200$ , this reduction is somewhat lesser,  $v_a = (0.5 \text{ to } 0.8) \times 10^4$  cm/sec; (b) sketches of the spots for July 6 and 7 show that the penumbra from the 6th to the 7th shrunk (in the N-S direction) by a value from 6.7 to 11.7 arc s (from 5.7 to 10.0 km per day) so that  $v_b = (0.7 \text{ to } 1.2) \times 10^4$  cm/sec; and (c) the distance on July 7 between spots a20 and S16 (they are also N26 and S25 for July 6) increased after the flare by 5 arc s; other spots display either lesser, or the absence, of shifts. Therefore,  $v_c \approx 0.5 \times 10^4$  cm/sec.

Analogous estimates were made from comparison of fields and groups on Sept. 1 and 2 (Figures 9 and 10); there, the region of S-polarity shrunk more in the E-W direction (the maximum shift of the  $H_{\parallel}$  line = 0.0 to 16 arc s), the remaining shifts comprise from 12 to 13 arc s, which gives  $v_d = (0.9 \text{ to } 1.2) \times 10^4$  cm/sec (interval between the maps is of 1<sup>d</sup>.12). For example, the distance between the spots S24 and S20 for Sept 1 varied by 12 arc s (spot S20-S18 for Sept 2), which gives  $v_c = 1.2 \times 10^4$  cm/sec. For other spots, the variations are even smaller and  $v_c = 0.9 \times 10^4$  and  $0.54 \times 10^4$  cm/sec (there was no substantial variation of the distances between the spots of Aug 31 and Sept 1). We note that the velocities of particle drift are of the same order and follow from Gopasyuk et al., (1963a) for a large number of groups with flares. The evaluation of the average radial velocities of motion  $v_{\parallel}$  associated with the flares follow from Gopasyuk (1964) where it was found that during the flares, the velocities of fluxes increased only in the region of the nucleus and penumbra of the spot, when outside of the spots they remained unchanged, not exceeding 100 to 150 m/sec (in the region of spots, the velocities  $v_{\parallel}$  do not exceed 300 m/sec, while during the flare they reach 0.5 km/sec and in certain cases 1 km/sec). In particular, in the July 6 and 7 group, the average values of the measured  $v_{\parallel}$  did not exceed 150 m/sec outside of the spots.

Thus, the whole combination of data as to the velocities of motion of plasma in groups of spots (in particular, the ones we have studied) showed that the plasma motion velocities at the level of measurement of the magnetic field did not exceed 100 to 150 m/sec. This means that

$$\frac{1}{c} [v \times H] \leq \frac{10^4 \times 10^2}{3 \times 10^{10}} < 10^{-4}, \quad (8)$$

considering the average field at the periphery of the region with such a motion as being equal to 100 gs. If one takes the region of a larger field, say isogausses  $10^3$  gs, then the contour length  $L$  enclosing the region will be correspondingly 5 to 10 times smaller so that Eq. (7) will be so many times larger, but the ratio of intensities Eqs. (7) and (8) will remain the same. Thus, in the case of strong flares (see Eq. (3)), the relation

$$\frac{1}{c} |\mathbf{v} \times \mathbf{H}| / E \approx 0.1, \quad (9)$$

while for weak ones this relation is of the order of unity. This means that in Eq. (6), one can neglect the second term and consider

$$E \approx E' \approx 3 \times 10^{-4} \text{ CGSE} \quad (10)$$

with an up to 10% accuracy for strong flares. In this case, the emf that we calculated in the contour ( $10^9$  v) is the actual emf inasmuch as the induction emf associated with motion is negligible. In both cases, both emf are of the same order; however, even in this case, the absence of emf in the lower layer (photosphere),  $E' = 0$ , does not mean that in the upper one (chromosphere) the same condition is satisfied since the plasma motions in the upper layer need not follow those in the lower and in principle may occur even in opposite directions. This will mean that in the upper layer (chromosphere), the emf occurs, when in the lower layer (photosphere) it is absent. This is helped by the decrease of the conductivity value  $\sigma$  in the chromosphere (see Eq. (6)).

The result of Eq. (10) on the other hand, because of Eq. (6), shows that the assumption of  $\sigma = \infty$  is unacceptable. Indeed, as long as Eq. (10) is realized, one can estimate how  $\sigma$  must be, since the value  $j$  must also be estimated from field  $H$  measurements. Indeed, measurements of the field gradient show (see above and also in Sec. 6) that

$$|\text{rot } H| \leq 1.0 \text{ gs/km} = 10^{-5} \text{ gs/cm},$$

and, consequently, the current density

$$|j| = \frac{c}{4\pi} |\text{rot } H| \leq \frac{3 \times 10^{10}}{1.26 \times 10} 10^{-5} = 2.4 \times 10^4 \text{ CGSE}. \quad (11)$$

Since  $1a = 3 \times 10^9$  CGSE, then  $|j| < 10^{-5} a$ , and the total current from the region having an area of about  $5 \times 10^8$  cm (characteristic for the structure of the picture

of currents) (see the works of Severnyi, 1965b) will be  $J \leq 2.5 \times 10^{12}$  a, as it is noted in these works. Consequently from Eqs. (6), (10), and (11) we obtain

$$J = \left( \frac{i}{E'} \right)_{\text{meas.}} \approx \left( \frac{2 \times 10^4}{3 \times 10^{-4}} \right) \approx 10^8 \text{ CGSE}, \quad (12)$$

which is three to four orders of magnitude below the usually accepted value ( $10^{11} - 10^{12}$ ). The fact that the conductivity must be theoretically three to four orders of magnitude lower than it was assumed up until now was also expressed in the works by Gopasyuk (1964) and Schroter (1964). However, this conclusion is a simple consequence of measurements.

Another experimental evidence of the final value of  $\sigma$  is the presence of motions across magnetic fields in the spot region and in the active regions (absence of freezing in), as follows from the works of Gopasyuk (1964 and 1967b). Apparently, as was observed also in the works of Severnyi (1960a), the tendency of flares to appear on the lines where the radial velocity  $v_{\parallel}$  disappears is not accidental, that is, where one can expect a strong drop of the induction emf  $\frac{1}{c} [\mathbf{v} \times \mathbf{H}]$  and where the total variation of the field flux leads to the actual appearance of the emf and possibly to the discharge.

The appearance of discharge and current around the active region and inside it, the possibility of which is indicated by the given evaluations of the actual emf, is based also on purely observational facts: before the flares, one frequently observes clearly fine bright and white (in the light  $H_{\alpha}$ ) filaments, passing through the active region (or surrounding it). With a good resolution, direct photographs of the flares in  $H_{\alpha}$  show their fine, well-spread-out filament structure (sometimes one observes a multitude of fine bright points or clouds) similar to the microstructure of the discharge\*. During the flares, bright large clouds appear frequently on the periphery of the active region, where already there is no noticeable magnetic field. If the flare process is associated with the discharge around the active region or through it (in the directions where the conductivity is maximum, in particular along the zero line), then the appearance of such clouds could be understood. In behalf of the explanations of flares by discharge phenomenon, the comparison of the location of flares with electric currents, performed by Moreton and Severnyi (1968) is ascertained, as well as the analogous comparison carried in Sec. 6 for the studied proton groups.

---

\*Reference can be made to the excellent photograph with high resolution performed by Bruzek et al. and already given in the just-published issue Mass Motions in Solar Flares and Related Phenomena, edited by Y. Ohman, *Novel Symp.* 9 (1968).

#### 4. POSITION OF FLARES RELATIVE TO THE LONGITUDINAL AND TRANSVERSAL MAGNETIC FIELDS

The first studied active region passing across the disk from 28 June to 10 July 1966 at the latitude of about  $33$  to  $35^{\circ}\text{N}$  and which gave a proton flare on July 7, occurred at the periphery of the old active region. In accordance with what was said in Sec. 2 about the magnetic configuration, two series of spots of opposite polarities aligned themselves here, almost parallel to the equator, and on July 5, the spots of opposite polarity were inside the common penumbra which is the characteristic property of the group with proton flares. Excellent photographs of the July 4 to 8 group were obtained by Steshenko (1968). The proton flare of importance 2b occurred on 7 July 1966 at  $0^{\text{h}}34^{\text{m}}$  UT. Prior to it, the flare activity was relatively weak: some activity was observed on July 6 when at  $5^{\text{h}}34^{\text{m}}$  and  $6^{\text{h}}34^{\text{m}}$  UT two flares of importance 1b and a series of smaller flares occurred. (All flares which occurred in the active region are given in Table 4.) Both of these flares were observed on the coronagraph KG-1 at the center of the line  $H_{\alpha}$  and also on both sides from the center at distances  $\pm 0.5 \text{ \AA}$ , which allowed the position of the flares relative to the spots to be determined quite accurately.

Surprisingly, all July 6 flares took place precisely in two small regions (within a few seconds). Such a picture was observed also on the next day, when a large proton flare occurred in the form of two large clouds located approximately in the same manner as the July 6 flares.

The second region passed across the disk from Aug 23 to Sept 3 at a latitude of  $22$  to  $25^{\circ}\text{N}$  and gave two proton flares: the first on Aug 28 at 15.21 UT (importance  $\geq 2$ :  $22^{\circ}\text{N}$ ,  $0.5^{\circ}\text{E}$ ) and the second on Sept 2 at 5.48 UT in a group of spots where, similarly to the case of the July group, one observed magnetic poles opposing each other — spots of opposite polarity, but the magnetic axis here was tilted by an angle of about  $45$  deg to the parallel.

We consider the position relative to the longitudinal and transversal field for which we possess original  $H_{\alpha}$  films namely, a series of flares on July 6 and 7, among them the proton flare at 0.26 UT ( $H_{\alpha}$ -film, which was obtained at the SibIZMIRAN), and also flares on Aug 30 to Sept 2,  $H_{\alpha}$ -films of which were obtained on the coronagraph KG-1, including the proton flare at 5.48 UT on Sept 2. The proton flare at 15.21 UT on Aug 28 was not studied, since we did not have in our possession the  $H_{\alpha}$  film of this flare. Since taking of  $H_{\alpha}$  films of the flares on KG-1 was performed in the center of  $H_{\alpha}$  by  $\pm 0.5 \text{ \AA}$ , this allowed us to reliably define the position of the flares relative to the group spots. With the corresponding enlargement, one makes a sketch — a map of a group of spots — with marks of polarity and strength of the spots, using photoheliograms (obtained on the AFR-2 at Simeis) and sketches of the groups obtained during regular determination of the magnetic

Table 4\*

Date, 1966	Time, UT		Coordinates		Importance	Remark
	Beginning	End				
7/4	03.06	08.31D	34N	10W	3 x s	
	09.00E	10.51	35	10	1n	
	11.55E	13.35	34	16	1n	
	14.10	20.12D	34	16	6 x s	
7/5	00.51	24.00	34	32	16 x s	
7/6	00.31	01.30D	34	34	1n	
	01.55E	02.09D	33	32	1n	
	04.14E	05.00D	34	35	sn	
	05.34	05.50	35	37	1b	KG-1
	06.34	07.20	34	36	1n	KG-1
	08.12	09.00D	35	39	1n	KG-1
	09.14	14.10D	35	37	1b	
	12.59	16.00D	35	38	3 x s	
	17.42E	19.00D	34	44	1n	
	19.36	21.00	31	47	sn	
	20.30	21.12	34	45	1n	
	21.10	22.55D	35	47	3 x s	
	7/7	00.26	02.39	35	47	2b
04.20E		06.00	36	48	1b	
08.00		10.00D	35	50	1n	KG-1
10.56E		-	35	50	1n	
11.15E		11.33D	35	50	1n	
11.50E		12.19D	35	50	1n	
12.22E		13.00D	35	50	1n	
13.20		-	35	50	1n	KG-1
18.17		20.17	35	60	4 x s	
21.32		21.50	34	61	1f	
8/26	08.20	15.48	21	28E	4 x s	
	17.28	19.00	24	22	2n	
	21.46	22.40	24	31	2n	
	23.15	23.52	24	22	sn	
8/27	02.10	02.40	24	29	sb	
	12.56	13.37	20	15	1b	
	16.00	19.10	22	13	4 x s	
	20.07	23.47	22	10	1n	
8/28	03.18	07.34	23	05	2 x s	
	09.00E	10.05D	25	02W	1n	
	13.09	13.22	26	03E	sf	
	15.21	20.00	22	05	≥2	
	16.40E	17.50	21	00	1n	
	18.18	22.55	22	01	5 x s	

\*The flares, identified by KG-1, were taken from observations of the Crimean Astrophysical Observatory; the flares, identified by SibIZMIR, were taken from observations of SibIZMIRAN; the others from Solar Geophysical Data (Boulder). For the combined sub-flares, the mean coordinates are indicated.

Table 4 (Contd)

Date, 1966	Time, UT		Coordinates		Importance	Remark
	Beginning	End				
8/29	05.35	06.43	22N	07W	1b	
	08.49	09.12	20	05	sn	
	12.06	12.33	21	10	1f	
	13.16	15.07	22	11	1b	
	14.54	19.21	22	11	3 x s	
	20.21	22.01	24	18	1b	
8/30	02.12	02.58	24	20	1b	KG-1
	11.37	12.44	23	23	1n	
	13.47	14.17	22	27	sn	
	14.50	16.21	23	27	2n	
	18.50	21.58D	25	25	4 x s	
8/31	00.02E	00.21D	22	30	1n	SibIZMIR
	00.36	02.35	22	30	2n	
	02.50E	04.21	22	28	2n	
	06.04E	06.20D	27	32	1n	
	09.48	—	22	37	1n	
	11.51	12.07	23	35	1n	
	12.53	13.50	22	40	1n	
	15.40	18.48	23	36	3 x s	
	18.35E	20.09	22	36	1n	
	20.13	21.30	22	43	3 x s	
	9/1	00.34E	11.05	22	45	
11.46		12.15	26	45	1n	
12.17		—	22	50	1n	
12.40		12.55	26	45	1n	
13.06		13.15	22	54	1n	
13.20		13.48	22	54	1n	
15.20		22.10	23	52	7 x s	
9/2	00.08	04.12	23	55	5 x s	KG-1
	05.48	—	24	56	3n	
	13.04	23.38	24	66	7 x s	

field of the spots on the horizontal solar telescope (see Koval' and Stepanyan, 1970). In addition, for both groups, we had several excellent photographs in white light on 35-mm cine-film\*, which was used to better define the structure of the group of spots and to compare fields with fine group structure. By projecting the  $H_{\alpha}$  film on the map of the spots (by means of superposition of the locations of at least three spots), and knowing the spot, one can fix the location of the flare inside the group utilized for the scanning of the active region (performed by means of the guide BST giving a 720-mm picture of the Sun) and knowing the direction of the daily parallel, we were able to fix the position of the flares on the maps of transversal and longitudinal fields.

\*This cine-film was kindly made available to us by N.V. Steshenko.

Usually the very initial phase of flare development was selected, when the flare consisted of separate bright points, well seen in  $H_{\alpha}$  as well as (sometimes) outside the band at  $\pm 0.5 \text{ \AA}$  from the center. For proton flares, certain (with the best picture quality) position of the flares in the maximum phase of development were fixed. As it is noted in the works of Moreton and Severnyi (1968), the error of such a method of fixing the location of flares consist of  $\pm 2$  arcs. Noticeable individual motion of the spots forced us to select sketches of groups and maps which were closest in time to the flare and to each other. The majority of the studied flares is shown in Figures 4 through 10. However, during thorough analysis of the flare location we: (1) studied also the sub-flares; and (2) could not make a strict comparison which can only be made by means of crosses in Figures 4 through 10, since for greater accuracy, other maps for the same day were selected which were closer to the instant of the flare and which presented greater interest. Therefore, the comparison which can be made with the help of Figures 4 through 10, even though providing in general a correct representation, will still not be detailed.

The locations of 17 bright knots were examined only for the first group of spots and 30 for the second, not including the long filaments and large clouds of proton flares in the maximum phase of their development. For the first group, maps were taken for  $\lambda 6103$  because of the great proximity of the level of this line to the chromosphere. For the second group, recordings in  $\lambda 6103$  were fragmental, and maps were selected for  $\lambda 5250$  only. The preference was furthermore given to the "green" photometer because of better focussing of the spectrograph camera in this case.

Further, as it was noted in Sec. 2,  $H_{\parallel}$  and  $H_{\perp}$  maps show a great similarity especially through a one day period, while the configuration of the spots sometimes changes noticeably during the day. Such a situation frequently permits a choice of one of the  $H_{\parallel}$  maps and one of the  $H_{\perp}$  maps as characteristic for the magnetic configuration of the given day, taking their proximity to the flare into account, and then use them together to form a combined map of the field containing certain characteristic isogausses ("hills") of the field  $H_{\parallel}$  and of the direction  $H_{\perp}$  (without indicating the length of the vector, if it exceeds 10 mm of potentiometer deviation). Such maps are most convenient for comparing the position of flares relative to the longitudinal and transversal fields; they were composed for July 6 and 7, Aug 31, and Sept 1 and 2 and were shown in Figures 18 and 19. They also show which maps (from Table 1) were used and that the flares are numbered.

Let us consider the position of the flares relative to the longitudinal field. Surprisingly, all flares of 6 July 1966, including 1b at 5.34 UT, accurately appeared simultaneously in the form of small bright formations in two and the same points, one in which B coincides with the neutral line  $H_{\parallel} = 0$ , and the other in which A extends across from the first point at a distance approximately 15 arc s from it

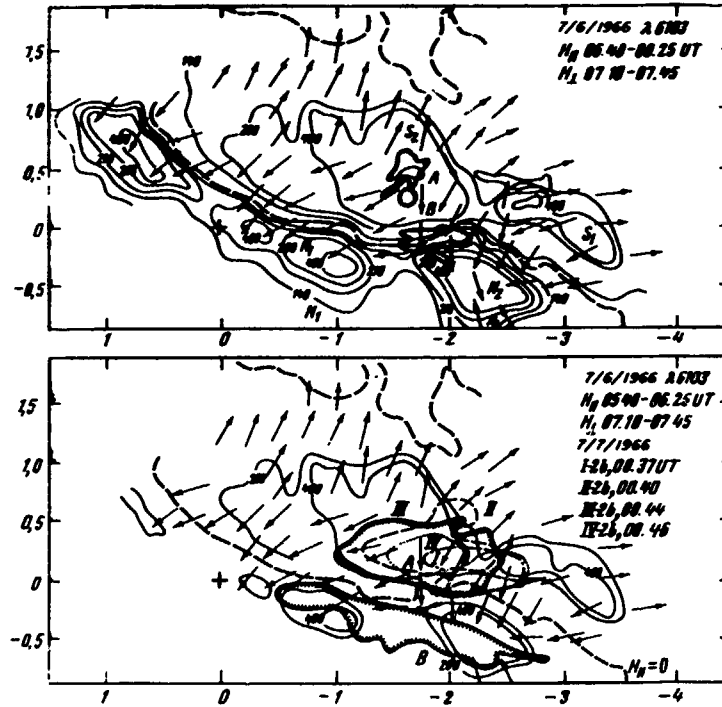


Figure 18. Comparison of the Maps of the Longitudinal  $H_{||}$  and Transversal  $H_{\perp}$  Fields With Locations of Flares for 6 and 7 July 1966 (denoted by hatched lines on the inner side)

northward, in the middle of the isogauss contour of S-polarity of greatest strength at the "top of the hill" (Figure 18, top). Both of these flaring regions occurred approximately at the same place where the bright regions also occurred and which were occupied by the proton flare of July (Figure 18, bottom). For the proton flare of July 7, we give its location at different times determined independently from different frames (the spots were poorly distinguishable on the  $H_{\alpha}$ -film) which, although not poorly coinciding with one another, show that even though the beginning of the flare is not recorded, the proton flare during the first minutes of its existence formed two gigantic shiny filaments, extended approximately along the neutral line (parallel to it) and located on both sides from it – one large cloud at the north and another thin filament to the south from the line  $H_{||} = 0$ .

As seen in Figure 18, the northern flare cloud was extending rapidly eastward with time (from 0.37 to 0.44 UT, displacement by 18.8 arc s). The displacement velocity of the eastern boundary of the cloud was

$$v = \frac{1.5 \times 10^4}{4.2 \times 10^2} \text{ km/sec} = 36 \text{ km/sec} .$$

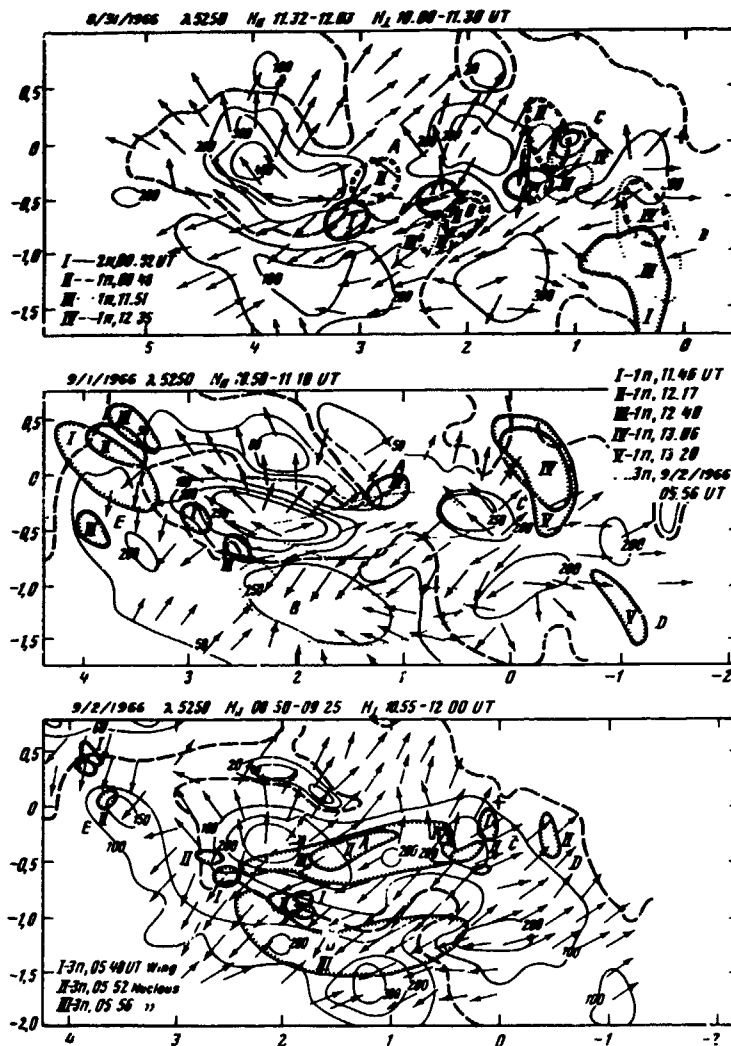


Figure 19. Same as in Figure 18 for 31 Aug and 1 and 2 Sept 1966

Apparently this process was not a real motion but rather an expansion of the excitation front, since after 2 min at 0.46 UT, a substantial part of the cloud to the east of the middle became extinct (it is possible that it left the band). The south filament of the flare broke into two at that time, although it is possible that loss of visibility in the middle of the filament was due to a fast ascension of the middle portion. (Let us note that the proton flare is intentionally plotted on the map of the preceding day to clarify the possible peculiarities of the field which preceded the proton flare.) Table 5 gives the distances (shortest) of the knots of A and B flares

Table 5

Flare, UT	$d_A$	$d_B$	Flare, UT	$d_A$	$d_B$
7/6/66			7/7/66		
4.32, end sm	10" N	1.2" N	0.37, 2b	1.9-5.0" N	3.7-0.4" S
4.52, sf	17" N	1.2" S; 0	0.40, 2b	3.1-9.4" N	3.7-9.4" S
5.08, 1f	14" N	3.1" S	0.44, 2b	3.1-9.4" N	3.1-9.4" S
5.34, 1b	17" N	0-1.2" S	0.46, 2b	2.8-6.2" N	3.1-11" S
6.34, 1n	11-17" N	0-1.2" S	Average	3.8-7.5" N	3.4-9.8" S
8.28, 1n	9" N	1.2" S	3.54	-	-
Average	14.4" N	0.4" S	8.00, 1n	4.4" N	-
			13.40, 1n	3.1-3.7" N	-

of July 6 and 7 from the neutral line. For the proton flare of July 7 at 0.26 UT, the largest and smallest distances of A and B filaments are given. On the average, as it is seen from Table 5, both extended clouds of the flare were located approximately symmetrically with respect to the line  $H_{\parallel} = 0$  at distances of 2.8 to 9.8 arc s from it in the regions of opposite polarity – a fact noted for other flares for the first time by Moreton and Severnyi (1968). Further, if one constructs a histogram for 17 knots of flares, contained in Table 5, one obtains a distribution (Figure 20, left) showing a grouping of values within two intervals: 0 to 6 arc s and 12 to 18 arc s

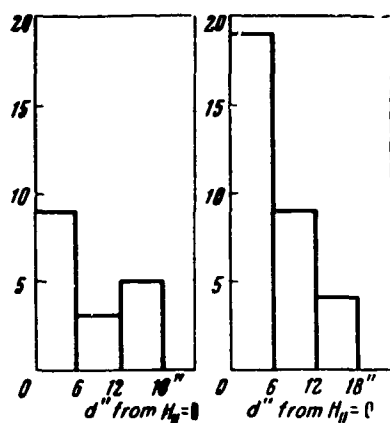


Figure 20. Histograms of the Locations of Bright Knots of Flares in the First and Second Active Regions Relative to the Neutral Line  $H_{\parallel} = 0$

The gradient of the longitudinal field at the neutral line in the region of flare occurrences of July 6 and 7 was

$$\left(\frac{\Delta H_{\parallel}}{\Delta s}\right)_0 = \begin{cases} 0.4 \text{ gs/km for } \lambda 6103, \\ 0.5 \text{ gs/km for } \lambda 5250, \end{cases}$$

that is, it was very large – typical for flares of this kind according to Gopasyuk et al (1963a).

A similar picture of location of flares can be noted also in the second group (Figure 19). On Aug 31, four sources of flares were active (denoted by A, B, C, and D on Figure 19). The first two of them, A and B, are located near the neutral line to the north and south of it. The Sept 1 flare occurs in the A and C regions: the source E also occurs.

On Sept 2, at the beginning of the proton flare, the first bright points appear immediately in the regions A, B, C, D, and E. The bright knots of the A and B flares, clearly visible at 5.48 and 5.52 UT, are located (B flare) on the neutral line  $H_{\parallel} = 0$ , and the other (A flare) to the north of it at a distance of about 15 arc s, which is approximately the same as happened before the proton flare of July . Shortly after, as for the July 7 flare, two powerful clouds formed in the center of the region; filaments are extended along the neutral line  $H_{\parallel} = 0$  (almost parallel to it). However, the northern one unites both sources A and C - occurrence of the first brightenings. In addition, extended clouds in the regions D and E occur also, but we will not give them because of the absence in these regions of variations of transversal fields. (The clouds usually appear at the periphery of the group and apparently are rather a secondary formation, even though first brightening of these clouds also happens to be well related to the neutral line  $H_{\parallel} = 0$ .) The formation of bright shiny ribbons on both sides of the magnetic axis of the group (parallel to the line  $H_{\parallel} = 0$ ) was also noted earlier for flares with cosmic rays by Severnyi (1963) and Ellison et al. (1961). Apparently this is one of the characteristics of proton flares.

The connection of the bright knots of the flares of Aug 31 to Sept 2 with the neutral line turns out to be closer than for the flares of the July group, as is shown from the histogram of Figure 20 (right); out of 32 knots, 28 are located at distances  $\leq 12$  arc s and 19 (60%) at distances less than 6 arc s. The Sept 2 proton flare occurred in the region with a longitudinal field gradient at the line  $H_{\parallel} = 0$

$$\left( \frac{\Delta H_{\parallel}}{\Delta s} \right)_0 = 0.13 \text{ gs/km for } \lambda 5250$$

a value smaller than for the July 7 flare, but typical for the occurrence of strong flares according to Gopasyuk et al. (1963a). It is possible that smaller gradients as well as smaller flux and energy  $H_{\parallel}^2 V / 8\pi$ , for this active region after Aug 30, are associated with the occurrence prior to that of strong flares (importance  $\geq 2$ , as for example, the flare of Aug 28) which lead to partial "discharge" of the stressed condition of the magnetic configuration.

Let us consider the location of flares relative to transversal fields, given also in Figures 18 and 19. For the first region prior to the flare of July 7, one observes a particularly characteristic picture: on July 6, the homologous flares A occur in the region of the radiant of the vector  $H_{\perp}$  directions, when flares B occur in the region where the directions of the vectors  $H_{\perp}$  intersect at a 90-deg angle, forming here a cross appearance made of vectors  $H_{\perp}$  going in directions E-W, and of vectors along the N-S direction (on the maps of  $H_{\perp}$  for July 7, this cross disappears at the site of the flares, and in the F region, one observes a flux of vectors

$H_{\perp}$  only in the E-W direction) (see Figure 12b). It is characteristic that this horizontal flux of  $H_{\perp}$  directions coincide practically with the neutral line  $H_{\parallel} = 0$  at the flares site B, which indicates a very peculiar field configuration.

Firstly, on one side of the line  $H_{\parallel} = 0$ , the longitudinal component is directed towards us and on the other away from us. Thus, in the region where the transversal component is parallel to the line  $H_{\parallel} = 0$  (to the left of B), we must have a contact of fields, crossing and tilted relative to the plane of the picture (Figure 21, left), such that on one side of the line  $H_{\parallel} = 0$ , H vectors are directed inwards, and

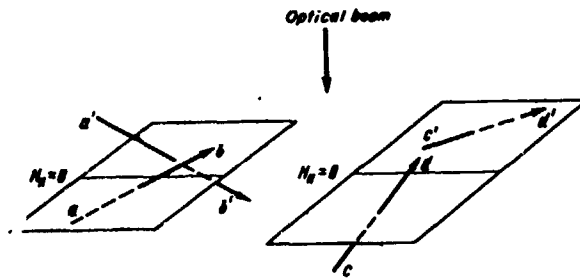


Figure 21. Diagram of the Possible Location of the Lines of Force in the Region of Bifurcation, 6 July 1966

on the other, they are directed outwards. Also, the transversal components of these fields  $ab$  and  $a'b'$  are approximately parallel to each other. Secondly, to the west of B, the picture is less complex and can be simply explained if the line of force forms one arc, the trace of which, in the plane of the picture, intersects the line  $H_{\parallel} = 0$  at approximately a right angle (Figure 21, right).

It is very difficult to imagine the combination of both pictures of the field to the left and to the right of B without making use of the concept of the fact that the lines of force responsible for the configuration on the left are located in the other plane, different from the plane where the lines of force are located which give the configuration on the right. Thus, the lines of force running along the line  $H_{\parallel} = 0$  ( $ab$  and  $a'b'$ ) pass in the other layer under the arc of line of force ( $cd$  and  $c'd'$ ). The horizontal directions of  $H_{\perp}$  which appear again just to the right of B verify this. An impression is created that the lines of force from the pole  $S_1$  partially close on the pole N passing "under" lines of force connecting poles S and N; that is, the closing of the lines of force does not go to the nearest pole but instead criss-cross, forming a typical case of wrong magnetic connection or misconnection.

In order to assure ourselves of the reality of such a picture, we superimpose the map of directions  $H_{\perp}$ , Figure 18, with the photograph of the fine structure of the spots, kindly put at our disposal by N.V. Steshenko (Figure 22). Aside from the field and fine structure filaments (possibly, because of the difference in time between the obtaining of the picture and the field and very fast variation in the group), one observes a very good correspondence almost everywhere. In particular, the joining of penumbra filaments oriented at a  $90^{\circ}$  angle to each other



Figure 22. Comparison of the  $H_{\perp}$  Directions (arrows) with Fine Structure of the Spot (penumbra filaments are dashed; flare regions are hatched)

correspond to the intersection of the fields  $H_{\perp}$  in the B region. Regarding our maps of  $H_{\perp}$ , if one could assume that their resolving power is small, and therefore, the intersection of  $H_{\perp}$  near B appears because of the low resolution, then the photographs of the spot are obtained with an excellent resolution quality of not less than 0.5 arc s. Therefore the intersection at a right angle of  $H_{\perp}$  directions in the B

region is a real effect, ascertained by a fine structure of the penumbra – the orientation of its filaments. Such a construction also reveals a multiple layer structure of the spot: to the left of B we see, let us say, a deeper layer with a magnetic field, which is sharply different (with a step) from the field to the right of B where we see a more peripheral layer with a field appropriate to it.

The region of intersection of the fields at B is a typical example of the region of "bifurcations" of the transversal field described by Severnyi (1964b) and Moreton and Severnyi (1968) where a strongly expressed tendency of appearance of flares in such regions (for example, 83% of all flares in the Sept 1963 group) is shown. It is necessary to note that the regions A and B are regions where one observes a strong transversal field; namely the following average values of  $H_{\perp}$  are typical for the region "under" the flare.

<u>Flare</u>	<u>A</u>	<u>B</u>
6 July 1966	910 gs	620 gs
7 July 1966	2000 gs	540 gs

Therefore, the regions under the flare cannot be regarded as neutral points or regions, as it has been pointed out for the first time by Michard et al. (1961) and Severnyi (1964b). It is also difficult to imagine a magnetic configuration for which the regions A and B would be neutral points, located above the photosphere (for further discussion about the absolute field, see Sec. 5).

A more diversified picture of the location of flares relative to  $H_{\perp}$  is observed for the second group. On Aug 31, all the sources A, B, and C are connected with the regions of "bifurcation" – intersection of  $H_{\perp}$  vectors (Figure 19). In regions B

and A, there is intersection of  $H_{\perp}$  vectors similar to that in the B region for July flares. At the source C, one notes the joining of  $H_{\perp}$  vectors of opposite directions. Characteristically, this region coincides with the closed region  $H_{\parallel} = 0$  which makes such a feature of the magnetic field similar to the neutral point. In the A region, there are two features of the field pertaining to B and C. On the map of Sept 1, one shows the locations of the flares for Sept 1 and the proton flare of Sept 2. Here also, one clearly observes the initial brightenings of the flares in A, B, and C, among which A is connected with the region where  $H_{\perp}$  vectors of opposite directions merge, C with a radiant of  $H_{\perp}$  directions, and in the B region, there occurs a strong rotation of  $H_{\perp}$  vectors from a direction close to W-E, to the south.

Let us now examine the location of the proton flare on the Sept 2 map. Here these "bifurcations" at A and C are clearly defined, as on Aug 31 and Sept 1. For E there is no sufficient data, but in D one notes only a small break in the trend of  $H_{\perp}$  directions. The smooth trend of  $H_{\perp}$  directions is observed in the B region, where one of the flare knots occurred. However, on Sept 1, prior to the flare in this region, one observes sharp rotations of the  $H_{\perp}$  vector, but it is known that the flares do not infrequently lead to vector rotations (see the work of Severnyi, 1964b). The Aug 31 and Sept 1 maps clearly show that the source of flares in B is connected with the crossing of  $H_{\perp}$  vectors at almost a right angle "bifurcation", characteristic apparently for the "intersection" of lines of force, running at different levels (associated with misconnection) as for the knots of the B flares of July 6 and 7. The  $H_{\perp}$  configuration associated with A and C on Figure 19 is similar to that for knots of the A flares of July 6 and 7. Large transversal fields are observed in the regions of appearance of the flares as is seen in Table 6. This apparently, as in the case of July 7 flare, excludes the possibility of simple identification of locations of flare appearance with neutral points in the photosphere field.

Table 6

Flare	A	B	C	D	E
31 Aug 1966	> 1000 gs	> 960 gs	520 gs	180 gs	-
1 Sept 1966	> 1000 gs	> 1000 gs	1300 gs	-	-
2 Sept 1966	760 gs	> 1000 gs	880 gs	-	600

The rotations of  $H_{\perp}$  vectors connected with the appearance of flares makes it possible to assume that the locations of appearance of flares are associated with the locations of a strong rotation of the  $H_{\perp}$  vectors with depth, which follows from comparison of  $H_{\perp}$  maps, obtained at two different lines (the effect as described by

Severnyi, 1964a). Simultaneous recordings in  $\lambda 5250$  and  $\lambda 6103$  allow us to construct the maps on which are simultaneously plotted the vectors  $H_{\perp}$  in these two lines, and the location of flares is given. Such maps were made for Aug 30 (13.40 to 14.35 UT), Aug 31 (two maps: 10.00 to 11.30 and 14.30 to 15.30 UT), and also for Sept 1 (8.07 to 8.50 UT). But the study of the location of flares on these maps has shown that there is no sufficiently well defined connection between the flares and the positions of strong rotations of the vector  $\delta_{\perp}$  during the passage from one level to another.

## 5. PROTON FLARES AND TOTAL FIELD STRENGTH

Ten isogauss maps of the total strength  $|H|$  were made on the basis of the observed maps of  $H_{\parallel}$  and  $H_{\perp}$  and empirical calibration (Severnyi, 1967) for the group of July 4 to 7, and four maps for the second group of Aug 30 and 31 and Sept 1 and 2\*. Examples of these maps on Figure 23 for the first active group show well the basic process which accompanies the development of magnetic configuration of such groups – the process of splitting up of a large cross-section of "monolithic" tubes of lines of force into smaller ones; this process was also recently observed in the works of Gopasyuk (1960).

One can also see from Figure 23 that the isogauss contours of a given strength at  $\lambda 4308$  are wider than for  $\lambda 5250$ . This indicates that the magnetic flux and the energy at the lower level are higher than at the upper one. The same can be obtained from planimetry of isogauss maps for  $\lambda 5250$  and  $\lambda 4808$ . Thus, we have  $|H|^2 V / 8\pi \approx 2 \times 10^{35}$  ergs for  $\lambda 4808$  when, for  $\lambda 5250$ , this value is of about  $2 \times 10^{33}$  ergs, if the volume  $V$  is the same. This can mean that  $|H|$  at the lower level is approximately 10 times greater than at the lower (sic) one. On the other hand, actual maximum values of  $|H|$  do not differ by more than a factor of three. Further maximum values of the field strength  $|H|$  at the upper level  $\lambda 6103$  are smaller by a factor of about three than the strength of the field at the level  $\lambda 5250$ . A difference by a factor of about ten between  $\lambda 4808$  and  $\lambda 5250$  obtained from energies  $|H|^2 V / 8\pi$  is therefore due to a greater area of the isogauss contours on the  $\lambda 4808$  map (greater by about three times). Thus, we see that the magnetic field of the active region is centered basically in the "deep" layers of the solar atmosphere.

The variation of the magnetic energy  $|H|^2 V / 8\pi$  for the first July group can be examined for the  $\lambda 6103$  level, for which we have maps for all three days, July 5, 6, and 7; the behavior of this value is shown in Figure 15; the increase of the energy up to  $6^{d4}$  is fully realistic. For  $\lambda 5250$ , we did not possess a map for

---

\*All these maps for the second region were first corrected for brightness.

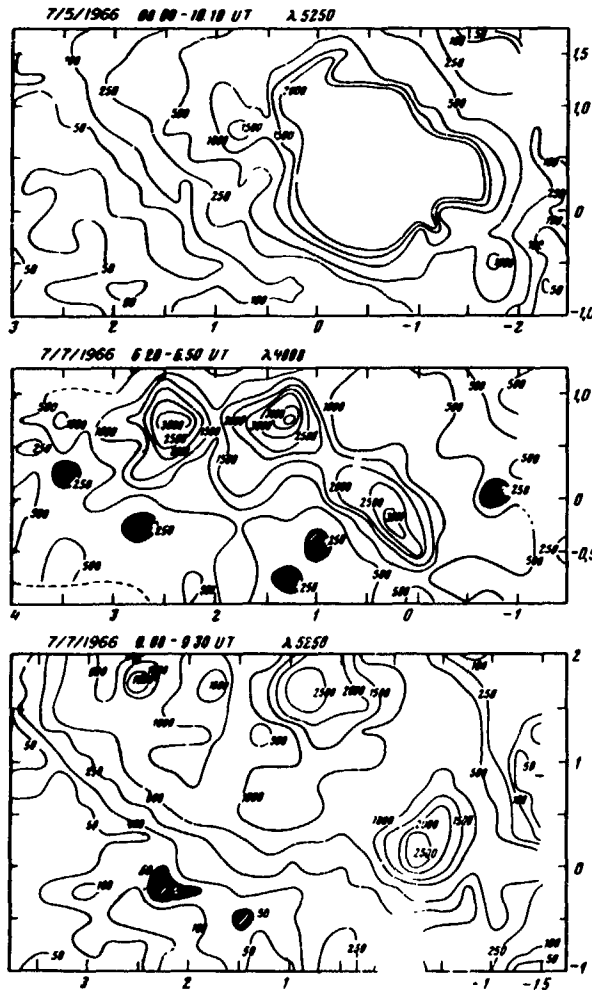


Figure 23. Example of Maps of Total Strength  $|H|$  at Different Lines for the First Active Groups. Hatched areas indicate "wells"

the second group, the maps of  $|H|$  field were made only for the four days, and the variations of  $|H|^2 V / 8\pi$  are also given in Figure 15, right. Here the energy value reaches  $12 \times 10^{32}$  ergs at a maximum on Aug 31 and Sept 1. That is, it is comparable to the energy of the first region, more precisely about two times smaller. However, the energy of the longitudinal field of the second group was four times smaller, which indicates a relatively greater role of the transversal fields in this case. We have for the first group (at the maximum)  $H_{||}^2 / |H|^2 = 3/4$ , when for the second group  $H_{||}^2 / |H|^2 = 20 \times 10^{31} / 10 \times 10^{32} = 2/10$ , that is in the first case, 75% of the energy was contained in the longitudinal field and in the second only 20%,

July 6, but comparison of data in Table 7 shows that the energy at this level prior to and after the flare is approximately equal, that is, that the initial value of  $|H|^2 V / 8\pi$  was re-established.

From the data of Table 7, we can also see that the energy of the upper level  $\lambda 6103$  is approximately three to four times smaller than the energy at the lower level  $\lambda 5250$ , which is basically associated with the drop in strength outward.

The following picture of the behavior of the magnetic field as a whole is the most likely: ascension of the configuration mass forces tubes upwards and then their lowering down. This will lead to a temporary increase of the energy and of the flux  $F_S + F_N$ . The possibility of such a process is indicated by the study of radial velocities in the active region prior to the flares and after them (Gopasyuk et al., 1963b). For

Table 7

Date, July	$\lambda$ , Å	$ H ^2 V / 8\pi$ , ergs	Date, July	$\lambda$ , Å	$ H ^2 V / 8\pi$ , ergs
5 <sup>d</sup> .34	5250	$10.1 \times 10^{32}$	7 <sup>d</sup> .36	6103	$6.45 \times 10^{32}$
5 <sup>d</sup> .39	5250	$22.1 \times 10^{32}$	7 <sup>d</sup> .39	5250	$17.7 \times 10^{32}$
5 <sup>d</sup> .39	6103	$4.02 \times 10^{32}$	7 <sup>d</sup> .41	5250	$20.9 \times 10^{32}$
6 <sup>d</sup> .28	6103	$11.9 \times 10^{32}$	7 <sup>d</sup> .43	5250	$15.5 \times 10^{32}$

while 80% in the transversal field. It is possible that this is connected with the fact that the configuration in the first case "went outside" to a greater degree than in the second, while the total energy is comparable in both cases (two times smaller in the second case). In addition, it is known (see Severnyi, 1964b) that at the edges of the field configurations, their field is basically transversal. In other words, one can assume that the second region (Aug - Sept) did not develop to such a stage which was reached by that of July, as a result of which there were no such strong and geoeffective flares as the July 7 flare.

Figure 24 shows isogauss maps for July 6 and 7 on which flares from Figure 18 are plotted; Figure 25 is the same and is plotted for the second active region for

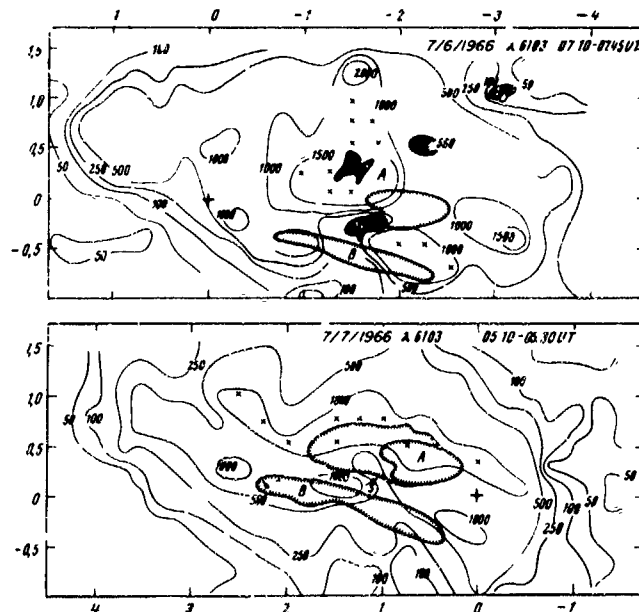


Figure 24. Location of the Flares of July 6 and 7, 1966 on the Maps of Total Intensity  $|H|$ . Crosses denote scaling region; wells are hatched; flares of the 6th are cross-hatched; flares of the 7th are denoted by hatches along the inner edge

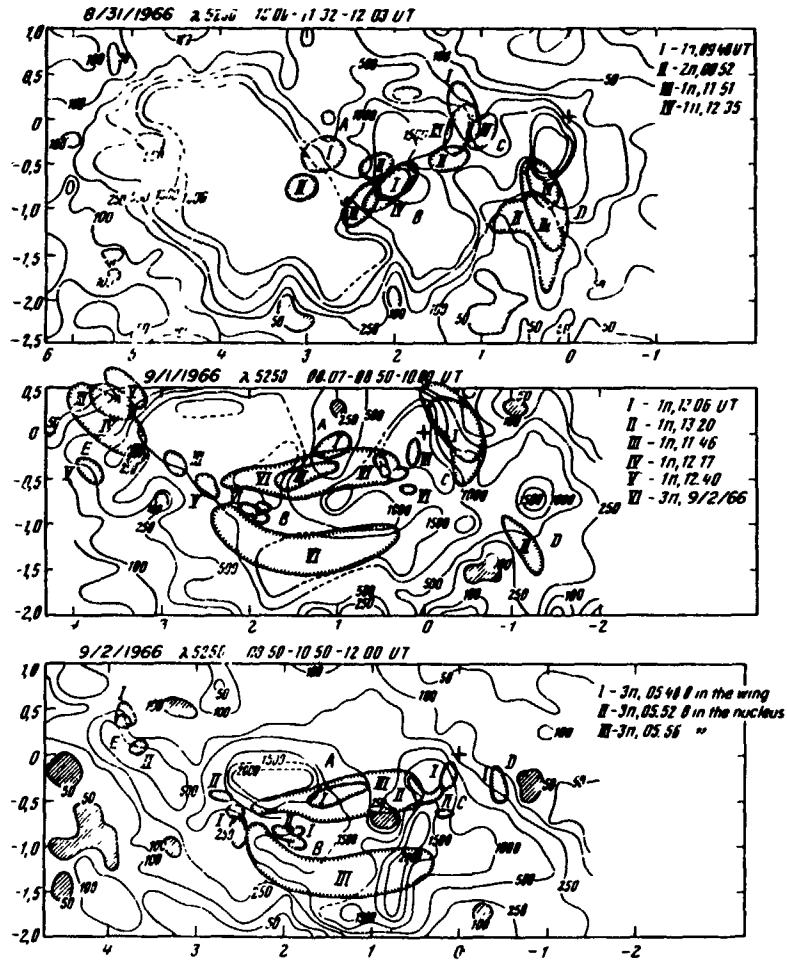


Figure 25. Locations of Flares of 31 Aug and 2 Sept 1966 on the Maps of Total Intensity  $|H|$ . Flares are hatched along the inner edge; wells are hatched completely

three days: Aug 31 and Sept 1 and 2, and the flares from Figure 19. The locations of flares on these maps are of interest. In particular, one cannot but note that the flares of the first region on July 6 and 7 occurred in the region where the gradient of the absolute field is maximum on the map of Figure 24, namely;

$$\Delta|H|/\Delta S = 0.37 \text{ gs/km for configurations of July 5,}$$

$$\Delta|H|/\Delta S = 0.74 \text{ gs/km for flares of July 6 and 7, 0.33 UT, and}$$

$$\Delta|H|/\Delta S = 0.25 \text{ gs/km for flares of July 7.}$$

One cannot but associate the occurrence of flares, in particular of the large p-flare of July 7, with a deep "ravine", reaching from the south the most powerful "pole" of the group (source B on July 6 and source A on July 7). At the same time, the source of the A flare of July 6 is above the region of the maximum absolute field.

Flares of the second group, in particular that of August 31, occurred in locations with large gradients of  $|H|$ , as is seen from Table 8. Their majority is located on the "slopes" of the hills of the field  $|H|$ .

Table 8

Date, 1966	Flare UT	Class	$\Delta H /\Delta S$ (for separate knots), gs/km	Date, 1966	Flare UT	Class	$\Delta H /\Delta S$ (for separate knots), gs/km
Aug 31	0.52	2n	0.52; 0.22	Sept 1	12.17	1n	0.24
	9.48	1n	0.22; 0.17		12.40	1n	0.1
	11.51	1n	0.62; 0.17; 0.18		13.06	1n	0.45; 0.22
	12.53	1n	0.56; 0.62; 0.17		13.20	1n	0.22
Sept 1	11.46	1n	0.34	Sept 2	5.48	3n	0.45; 0.32; 0.50; 0.23

Thus, the conclusion on the appearance of flares in regions of large gradient of the longitudinal field  $H_{||}$  remains justified also for the total field: the flare has a tendency to occur in regions of larger (greater than 0.1 gs/km) gradient of the absolute field.

From the study of the maps in Figures 24 and 25 (especially for Sept 2), one can suspect the connection between the occurrence of the flares with field "wells" - regions where the field strength has a minimum or drops to the noise level  $\sim 100$  to 200 gs. However, even if we assume as "coincidence" the difference in the location of the flare from the location of such a well by not more than  $d \approx 10$  arc s we do obtain the following statistics for the second active region, richer in the sense of a difference of locations of flares and knots:

Date	Number of Coincidences ÷
	Total Number of Knots
31 Aug 1966	1/14
1 Sept 1966	2/10
2 Sept 1966	2/6

We see that at the best (Sept 2), only 30% of the initial brightening of the flares takes place at distances of 9 to 10 arc s. All others are at a distance considerably greater from these "wells" of the field or zero regions. In a series of cases, brightenings such as A for Sept 2, source B and C for Aug 31, do not in general have any "wells" in the vicinity, and the source of A flares of July 6 and 7 occurred above the region of maximum strength of the absolute field.

All this points to the absence of any tendency for flares to occur in regions of minimum or zero of the field total vector, that is, to the absence of connection of the flares with real neutral points of the magnetic field of the photosphere. Also, one does not find such a connection for the flares which occurred in the group of 17 to 24 Sept 1963, studied by Moreton and Severnyi (1968). In these cases, when in the vicinity of the flare, there is such a sharp drop of intensity as for the source B of the July 6 and 7 flares one must rather suspect a connection of brightenings simply with a very strong field gradient, although in principle the possibility of neutral points is not excluded in this case. However, one would need far too many neutral points to explain all the observed brightening of the flare (as it was first noted by Kiepenheuer, 1965). On the other hand, it is very difficult to conceive of field configurations in which the neutral point would be located above the region of large  $|H|$  in the chromosphere.

Thus, the presence of strong transversal fields on the lines  $H_{\parallel} = 0$ , as well as the occurrence of flares in the regions of large values of  $|H|$ , makes us doubt the idea of an important role played by the neutral points in the appearance of solar flares.

#### 6. PROTON FLARES AND ELECTRIC CURRENTS. AMPERE FORCE AND RADIAL VELOCITIES

The occurrence of flares in locations with a large gradient of the longitudinal field and in "bifurcation" regions — regions with fast, sometimes jumpy (flare of 7 July 1966) variation of the direction of the transversal field  $H_{\perp}$  — points again to the possible connection between the appearance of the flares with locations of strong electric field where the current density

$$j = \frac{c}{4\pi} \text{rot } H$$

is sufficiently large. As in the work of Moreton and Severnyi (1968), for all the  $H_{\perp}$  maps indicated in Table 1, the maps giving the distribution of the vertical current component  $j_z$  from the maps of  $H_{\perp}$  ( $H_x, H_y$ ), were calculated using a computer

"Minsk-1."\* These distributions were compared among themselves and with the location of the flares.

For the first proton flare, the maps of  $j_z$  for July 6 and 7 are given in Figure 26. Only one recording of  $H_1$  for  $\lambda 6103$  is available for the 6th. Thus the

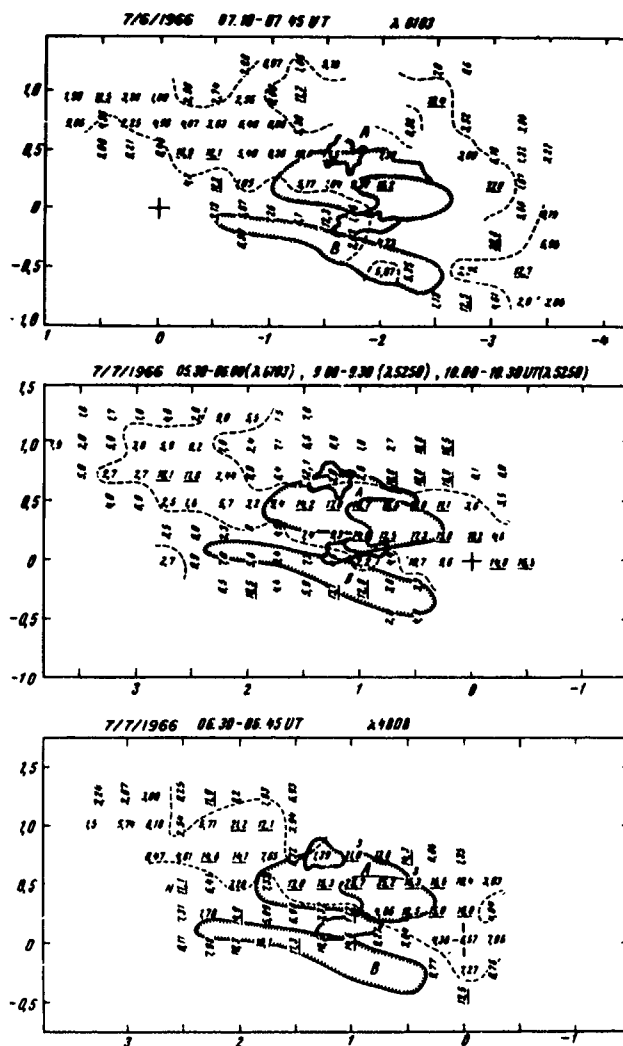


Figure 26. Map of Electric Currents  $j_z$  for July 6 and 7 and Location of the Flares (hatched along the inner edge) on Them. The  $j_z$  unit is  $10^{-2}$  gs/km;  $(+j_z)$  = horizontal numbers,  $(-j_z)$  = vertical numbers

\*The authors are indebted to T.G. Buslavskaya for performing the majority of these computations.

unique map of  $j_z$  (Figure 26, top) and for the 7th, there was one recording of  $H_{\perp}$  in  $\lambda$  6103, two in  $\lambda$  4808, and two in  $\lambda$  5250. Recordings (in the morning in  $\lambda$  6103 and two at noon in  $\lambda$  5250) are very similar with the same one in the other two, but for the sake of illustration, we give this map (Figure 26, bottom). On all three maps, flares are shown which occurred on the 6th and the proton flare of July 7. The study of their location clearly shows a close relationship of the source of flares A with the strongest current  $j_z$  of the same direction and source B with the strongest current in the other direction. (Flares of July 6 are better compared with the map of current  $j_z$  for July 6.) The difference in the location of the center of the bright knot from  $j_{\max}$  by 6 arc s can be fully attributed to measurement errors. As to the lower filament of the B proton flare, it is more correct to say that it passes through locations  $j_{\max}$  since we do not know the locations of the first brightenings.

For the second active region which gave the proton flare of 2 Sept 1966, the picture is not so simple (Figure 27) as for the flares of July 6 and 7. So, on Aug 31 the sources of homologous flares A, B, and D practically coincide with the locations of the relative  $j_{\max}$ , but the flares C are clearly displaced (approximately by 10 arc s) eastward from the relative currents maximum. Perhaps, this is the single case among all the ones considered so far in this work and in the work of Moreton and Severnyi (1968) when one observes a serious deviation. It is possible that it occurs because of the difference in time of obtaining the map and the time of flare appearance: flares which occurred close to the instant of field recording, namely II and III, reach closely with their upper end (at a distance  $\leq 6$  arc s) the region of  $j_{\max}$ .

It is of interest to note that the B flares occur in a very narrow interval between positive and negative maxima of  $j_z$  as if they appeared at the top of a current loop emerging from the point -17.6 and entering at point +17.0.

On Sept 1, positive and negative currents  $j_z$  coincide well with the source C of flares IV and V and also source E of flares I, II, and III, although here there is no sufficient data on the values of  $j_z$  at the boundary E of the map. For the first brightenings and clouds I and II of the proton flare of Sept 2 (5.48 to 5.25 UT), the picture is quite sharp: sources A, B, and C were the first brightenings to occur and correspond well to maximum values  $j_z$ ; however, it is difficult to judge of small brightenings in E since the values of  $j_z$  are insufficient here. If one uses the data of the  $j_z$  map for Sept 1, then these fine brightenings in the region E occurred near the maximum values of  $j_z$ . Thus, with the exception of two sources, C for Aug 31 and A for Sept 1, the remaining bright knots of flares coincide well with  $j_{\max}$  (within the measurement error limits of  $\sim 6$  arc s). Furthermore, statistics for both proton flares and flares preceding them are given below.

Period	Percent of Coincidence
4 to 7 July 1963	6/6
31 Aug to 2 Sept 1966	17/23

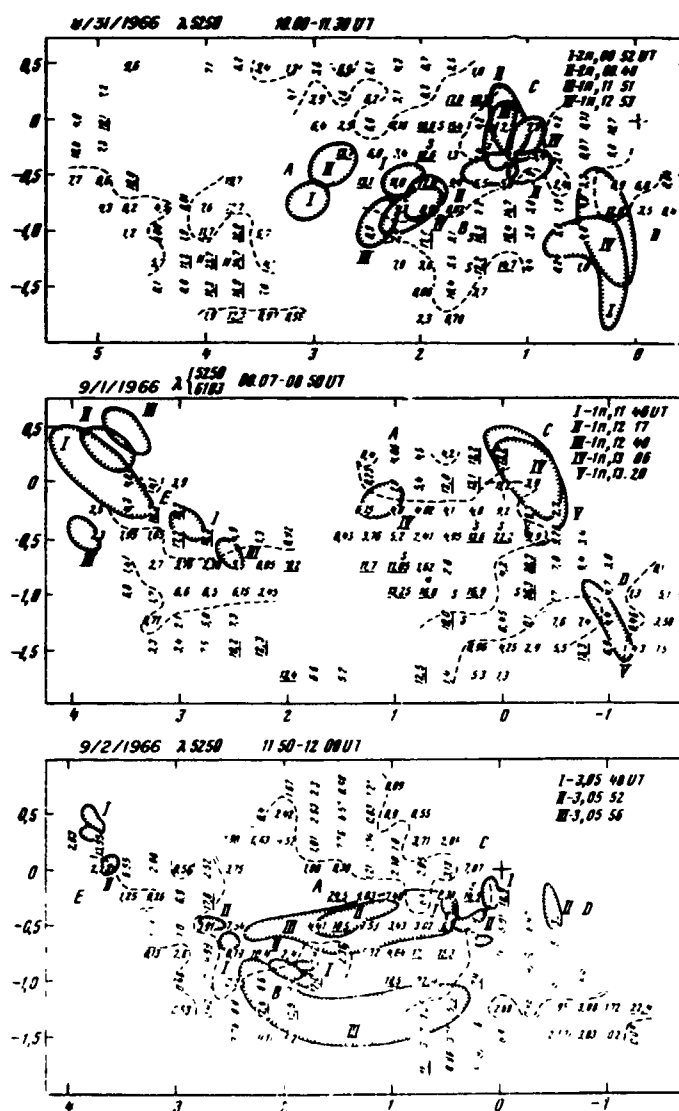


Figure 27. Location of the Flares on the Maps of  $j_z$  for the Second Active Region (Aug 31 and Sept 1 and 2). Notations same as in Figure 26

It follows from here that not less than 74% of all first brightenings coincide with the locations of the relative maximum  $j_z$ . In some remaining cases, where there is  $j_{\max}$  but the flares did not occur, the spots umbra is located where it is most natural to expect a very strong rotation of  $H_{\perp}$  and strong (at the boundary of the spot) fields  $H_{\perp}$ ; these locations must be excluded. Taking into consideration these extreme cases, we find for the second active region  $17/82 \approx 20\%$  of cases where at the location of  $j_{\max}$  the flare is not recorded and there is no spot.

However, one must also consider that flares and  $j_{\max}$  must be compared only in a limited interval of time, approximately in the limits of  $\pm 12$  h when there is no strong variation of the  $H_{\perp}$  field.

One must, finally, note an interesting tendency of occurrence of flare brightenings such that at least one of the flare knots corresponds to the sign of  $j_{\max}$ , opposite to the sign of all other knots, an effect which was also noted by Moreton and Severnyi (1968).

Let us note that the criterion of "strong" current, assumed here, is the same as the previous one by Moreton and Severnyi (1968), namely the "strong" corresponds to gradient  $\geq 0.1$  gs/km or to a total current  $J \geq \sim 5 \times 10^{11}$  amps.

The recordings of longitudinal  $H_{\parallel}$  and transversal  $H_{\perp}$  fields performed in two separate cases, simultaneously on two levels ( $\lambda 5250$  and  $\lambda 6103$  - level difference 160 km) allow us to also determine the transversal electric field  $j_{\perp}$ , the components of which  $j_x$  and  $j_y$  are

$$\begin{aligned} \frac{4\pi}{c} j_x &= \frac{\partial H_z}{\partial y} - \frac{\partial H_y}{\partial z}, \\ \frac{4\pi}{c} j_y &= \frac{\partial H_x}{\partial z} - \frac{\partial H_z}{\partial x} \end{aligned} \quad (13)$$

and can be found from maps of  $H_{\parallel}$  and  $H_{\perp}$  (recorded one after the other) for two levels ( $\Delta z = 160$  km). Calculations show that the basic increase of  $j_x$  and  $j_y$  is given by the derivatives of  $H_{\perp}$  with respect to depth  $z$ ; that is, the horizontal (transversal) currents are determined by the rate of change of  $H_{\perp}$  with depth, while the vertical currents  $j_z$  are determined by the rate of change of  $H_{\perp}$  in the plane of the picture. For example, for one of the characteristic points of the maps of current  $j_{\perp}$  for 7 July 1966 obtained from recordings in  $\lambda 6103$  (5.30 to 6.00 UT) and  $\lambda 5250$  (9.08 to 9.30 UT), we have

$$\begin{aligned} j_x &= +2.37, & \frac{\partial H_z}{\partial y} &= -0.046, \\ j_y &= -4.37, & \frac{\partial H_z}{\partial x} &= 0.0040, \end{aligned}$$

that is, the main contribution to  $j_{\perp}$  is provided by the gradients  $\partial H_y/\partial z$  and  $\partial H_x/\partial z$ . In general, for the majority of points one obtains on the average,

$$\frac{\partial H_{\parallel}}{\partial l} = \frac{\partial H_x}{\partial x} \sim \frac{\partial H_z}{\partial y} \approx \frac{200 \text{ gs}}{5 \times 10^3 \text{ km}} = 0.04 \text{ gs/km} = 0(10^{-2} \text{ gs/km}),$$

$$\frac{\partial H_{\perp}}{\partial l} = \frac{\partial H_x}{\partial x} \sim \frac{\partial H_x}{\partial y} \sim \frac{\partial H_y}{\partial x} \frac{\partial H_y}{\partial y} \approx \frac{2000 \text{ gs}}{5 \times 10^3 \text{ km}} = 0.4 \text{ gs/km} = 0(10^{-1} \text{ gs/km}), \quad (14)$$

$$\frac{\partial H_{\perp}}{\partial l} = \frac{\partial H_x}{\partial z} \sim \frac{\partial H_y}{\partial z} \approx \frac{650 \text{ gs}}{160 \text{ km}} = 4 \text{ gs/km} = 0(1 \text{ gs/km}).$$

Thus: (1) the variation of the longitudinal field in the plane of the picture is approximately ten times lower than that of the transversal field which is a natural consequence of a large inhomogeneity of the transversal field rather than of the longitudinal (for example, in the spot,  $H_{\perp}$  turns by 180 deg within only a few seconds, while  $H_{\parallel}$  smoothly reaches the maximum); and (2) the variation of the transversal field with depth  $\sim 1 \text{ gs/km}$ , as it is known from a series of works including that of Guseinov (1970), is considerably stronger than the variation in the plane of the picture and indicates a large field inhomogeneity with depth. This inhomogeneity also follows from the strong rotations of the vector  $H_{\perp}$  in separate locations of groups of spots (see works by Severnyi, 1964a). Considering the given situation, it results in the fact that the horizontal current densities  $j_{\perp}$  must be greater by an order of magnitude than the vertical ones  $j_z$ . However, since the dimensions of the regions occupied by the currents, approximately  $10^7 \text{ cm}$  is about ten times smaller than the regions occupied by the  $j_z$  currents, then the total current  $J = Sj$  ( $S$  is the region area) is of the same order in both cases.

In practice, the map of  $j_{\perp}$  is obtained as follows: first, the maps of  $j_x$  and  $j_y$  are made using reliable relationships (with an accuracy of about 1%) ( $\Delta z = 160 \text{ km}$ )

$$j_x = -\frac{c}{4\pi} \frac{\partial H_y}{\partial z}, \quad j_y = +\frac{c}{4\pi} \frac{\partial H_x}{\partial z}, \quad (15)$$

then one finds the value

$$j_{\perp} = \sqrt{j_x^2 + j_y^2} \quad (16)$$

(usually in units of  $0.5 \times 10^{-2} \text{ gs/km}$ ) and the map of the distribution of the vector  $j_{\perp}$  having projections Eq. (15) and length Eq. (16). The map of  $j_{\perp}$  for July 7 is shown in Figure 28. The location of two large (A and B) clouds of the proton flares at 0.44 UT is also given there. In the picture of the horizontal electric currents, the

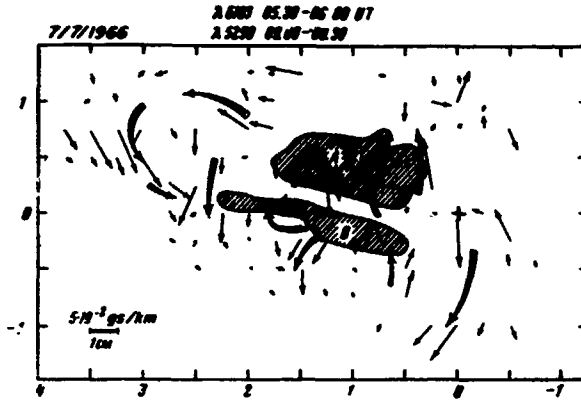


Figure 28. Map of Transversal Fields  $j_{\perp}$  for July 7 and Location on It of Clouds of the A and B Proton Flares (hatched)

contact of opposite currents in the middle of the map at the location of occurrence of the proton flare is characteristic. It is possible that two or three gigantic loop currents merge there as is schematically shown on Figure 28 by large arrows.

The picture of transversal fields in the active groups will be considered later in more detail. We show here the possibility and the usefulness of such a study, in particular

for the understanding of those forces which can act on the flare plasma from the side of the magnetic field. Indeed, knowing the components  $j_x$  and  $j_y$  of the current, one can compute the vertical component of the force  $F = j \times H$ , which, according to Eq. (15), will be:

$$F_z = j_x H_y - j_y H_x \approx -\frac{c}{4\pi} \left[ H_y \frac{\partial H_y}{\partial z} + H_x \frac{\partial H_x}{\partial z} \right]$$

$$= -\frac{c}{8\pi} \frac{\partial}{\partial z} (H_x^2 + H_y^2) = -\frac{c}{8\pi} \frac{\partial}{\partial z} H_{\perp}^2, \quad H_{\perp} = \sqrt{H_x^2 + H_y^2}. \quad (17)$$

The value  $H_{\perp}^2/4\pi = p_m$  is the magnetic pressure. In the plane of the picture, the positive x-axis is directed to the left, and the y-axis downwards so that the positive z axis is directed outwards, along the radius of the Sun. Therefore, if the gradient of the magnetic pressure

$$\frac{H_{\perp}^2(z_2) - H_{\perp}^2(z_1)}{z_2 - z_1}, \quad z_2 > z_1$$

is negative (pressure at the lower level greater than at the upper), then the force  $dp_m/dz < 0$  is against the gravitational force ( $-dp/dz = g_p$  in our case), and  $F_z$ , according to Eq. (17), is positive; that is, for  $F_z > 0$  the force is directed upwards (away from the surface of the Sun), and for  $F_z < 0$  the force is directed downwards (towards the surface of the Sun). The maps of  $H_{\perp}^2$  for two levels  $\lambda 5250$  (bottom) and  $\lambda 6103$  (top) are practically calculated, and the map of  $F_z$  is then made,

which is shown in Figure 29 for July 7; there the location of the proton flare is also shown. The regions of force acting downwards are found at the ends of the extended clouds of the flare, when in the middle of these filaments the force acts upwards so that the flare filaments intersect the line  $F_z = 0$ . This shows that the middle portion of the flare can ascend, when both ends descend; that is, a motion can occur which is in fact frequently observed in the flares on  $H_\alpha$  films, as well as spectroscopically, such as flow of matter along the arcs for a certain lifting of the arc. Analogous motions are similarly observed in loop prominences. Further, simple calculations show that the force  $F_z$  in the region of the flare is approximately ten times greater than the gravitational force or the gradient of the gas pressure.

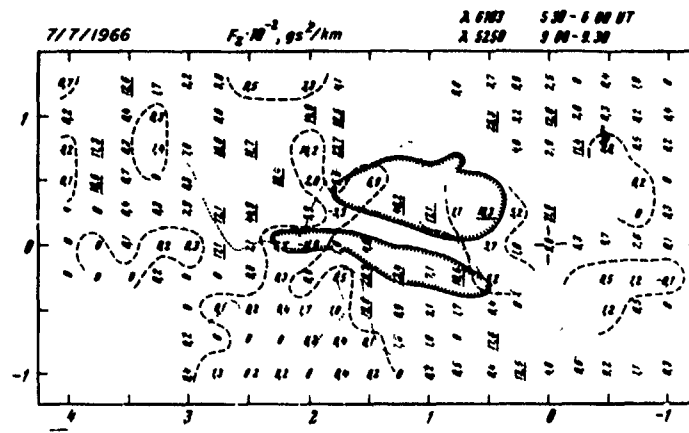


Figure 29. Location of Proton Flare on the  $F_z$  Map for July 7 (hatched along the inner edge).  $F_z$  line is dashed;  $v_{\parallel} = 0$  line is dotted

It is of interest to compare the distribution of the sign of the force  $F_z$  and the sign of the radial velocity recorded simultaneously with the recording of the longitudinal field (5.10 to 6.25 UT). Recording of  $F_z$  relates to the average moment, somewhat later (5.30 to 6.30 UT). The difference of the average times (5.46 and 7.30 UT) of both recordings can have a substantial value because of the periodic pulsations and faster velocity variations with time than those of the field. The comparison shows that the region of the positive force  $F_z$  and rise, in general, can be superimposed even though there are deviations. However, this interesting question must be studied, making use of a large number of data specially obtained for this purpose.

## 7. CONCLUSIONS

The present article is the seventh of the works performed in the past ten years at the Crimean Astrophysical Observatory on the study of magnetic fields associated with solar flares. Previous investigations have included the works by Severnyi (1958, 1960 and 1964b) (based only on the investigation of longitudinal fields), Howard and Severnyi (1963), Moreton and Severnyi (1968), and Gopasyuk et al. (1963a). It will be perhaps appropriate to review the results of this 10-year study, since in the majority of the cases the latest works reproduced to a significant degree in the new material the results obtained earlier. Furthermore, analogous investigations which took place at home and abroad together with the verification of the previously obtained results have made a substantial contribution which has influenced the further development of our work.

Spectroscopic and cinematographic investigations of flares, "moustaches", and other non-stationary phenomena (performed from 1948 to 1956 at the CrAO) led from 1956 to 1957 (Severnyi, 1956 and 1957) to the conclusion that, in speaking of energy in the atmosphere of the Sun, it is difficult to find an energy source other than the energy of the magnetic field capable of providing the actually observed energy radiation during flares in the form of cosmic ray energy as well as mechanical energy, thermal energy, and radiation energy (up to  $10^{32}$  ergs per flare). This made one begin, in 1957, the search for a relationship of the flares with the actually measured magnetic fields on the Sun. The fact itself of the appearance of flares almost exclusively in groups of spots — these basic carriers of solar magnetism — is a deciding factor in behalf of such a relation. (Even though later cases were found of the appearance of flares outside of spot groups, those were always regions of increased field strength.) Systematic (from 1957) discrete measurements of the magnetic field of individual spots as well as systematic total scanning of the active regions by means of a magnetograph were considered extremely important. Indeed, they allowed us to collect a unique material which accounts at the present time for no less than 800 recordings of the magnetic field in the active regions, particularly where the flares occurred. Only a small portion of this material was analyzed and studied in the previously mentioned seven works and also in the works by Martres et al. (1968b).

First, (in 1957) when one had only the data on the longitudinal fields and  $H_{\alpha}$  cine-films, it was found that flares occur very close to the zero line  $h_{\parallel} = 0$ , or coincide with the line of separation of polarities if in the vicinity there are at least three poles (hills  $H_{\parallel}$ ) or spots of different polarities. At this time, it was also discovered that after the flare, the isogauss density in the region of the flare decreases, the magnetic structure seems to be expanding, and the density of lines of force decreases. Ten years later, analogous effects for the flares of 21 and

23 May 1967 were observed by Tandberg-Hanssen et al., (1968). In 1959 (Severnyi, 1960b) verified a close relationship of bright knots of flare 61 with the line  $H_{\parallel} = 0$  and large gradients  $\nabla H_{\parallel} > 0.1$  gs/km. From the comparison of the magnetic maps of  $H_{\parallel}$  prior to and after the flare, the analogous effect of simplifying the structure of the field, of decreasing the field gradients from values  $\geq 0.1$  gs/km prior to the flare to values of about 0.01 to 0.02 gs/km after it for seven out of eight flares was found.

In the following work, Gopasyuk et al. (1963b) have studied the location of 51 powerful flares in groups of spots with measured field strength prior to and after the flare. Data of location, field strength, and areas of spot allowed us to also analyze the values of the field gradients near the neutral point of a certain equivalent dipole configuration having properties similar to those of the actual group of spots. (The comparison criteria were based on the facts that such properties of the actual field as the distribution of the field strength and inclination of the field vector in real spots are similar to those which are typical for dipoles or solenoids, if one decreases the scale of distances by  $10^8$  to  $10^9$  times, and the intensities by approximately ten times when going from the Sun to the laboratory.) In the works of Gopasyuk et al. (1963b) the statistical dependency of the power of the flare on these gradients was found: gradients greater than 0.1 gs/km were found typical for all proton and strong flares. This dependency was utilized for prognosis of flares which significantly helped in the selection of the periods of more frequent measurements of magnetic fields before and after the flares.

A close relationship of the flares with high field gradient was then found at the Meudon observatory, where instead of the gradient one used the ratio  $d/D$  ( $d$  is the distance between the spots,  $D$  is the diameter of the spot) (Avignon et al., 1964, 1966; Caroubalos, 1964). Only very recently this relationship was also ascertained by extensive investigation (Smith and Ramsey, 1967) at the Lockheed observatory.

The location of flares that we found (Severnyi, 1958 and 1960b) near the zero line  $H_{\parallel} = 0$  between hills, poles (spots) of opposite polarity (which leads to a large gradient of the field in the region of flare) has revived a number of attempts to explain flares as a result of plasma instability in the region of neutral points, occurring either during the shifting of "sources" of the field — poles, or increase of their intensity or other reasons (see Severnyi, 1958; Severnyi and Shebanskii 1961; Severnyi, 1962a; Sirovatskii, 1966); even before the actual measurements of the field, such an idea was first expressed in the works of Sweet (1958). It was, however, shown (Parker, 1963) that the mechanism of Joule losses under any processes in the vicinity of neutral points is non-efficient. The possibilities of dynamic dissipation of the field near the neutral point are proposed in the works of Sirovatskii (1966). The development of the hypothesis of neutral points continues to remain the center of attention up to now (Sirovatskii, 1968).

However, Michard et al. (1961), by means of direct spectral measurements and independently from the works of Severnyi (1964b) and (1962b) by means of a magnetograph, observed first strong transversal fields in the region of occurrence of flares, even if they lay on the line  $H_{\parallel} = 0$ . It was found that the transversal fields  $H_{\perp}$ , as well as the filament structure of the chromosphere in the line  $H_{\alpha}$ , which well reflected the structure of those fields at the locations of solar flares (Severnyi, 1962b) reveal intersection or "merging" of fields of different directions, the contacts of the oppositely directed vectors  $H_{\perp}$ , and other similar features called "bifurcations" (Severnyi, 1964b). It was found by Moreton and Severnyi, (1968) that the connection of the flares with regions of such peculiar behavior of the transversal field is as close as it is with the line  $H_{\parallel} = 0$ . Furthermore, in the works of Severnyi (1964b) and Moreton and Severnyi (1968), it was found that the flares appear simultaneously in the form of several bright spots - knots in different locations of the active region (which was known earlier), but such that these points are located in regions of opposite polarity. And if the significant part of them adjoins to the neutral line, then the remaining ones occur in the region of strong longitudinal field, sometimes near or at the top of the magnetic hill  $H_{\parallel}$  (boundary of the spot nucleus).

Similar cases are well expressed on 21 and 22 June 1962 (Severnyi, 1964b) 17 Sept 1963 (Moreton and Severnyi, 1968), 6 July 1966 (source B), 2 Sept 1966 (source B) in the present work and in a series of other cases. These results were ascertained by a very large amount of material on 57 active regions comprising 75 flares in the works of Martres et al. (1966). The present work ascertains again and completes this picture, showing that there is no connection between the flare location not only with real neutral points of the total magnetic field, but even with relative minima of this field - "wells" of the field, as it was expected from the theory developed by Wentzel (1964).

Thus, the collection of the observational data obtained so far leads us to take a critical view of the theory on the connection of the flares with instability in neutral points, which we have some time ago actively defended (Severnyi, 1958; Severnyi and Shebanskii, 1961; Severnyi, 1962a), and which is being actively developed by Sirovatskii (1968); it encounters very serious difficulties (see Parker, 1968).

At the same time, in the present work again as well as in the work of Moreton and Severnyi (1968), the connection of flares with the electric currents calculated from Maxwell's equation  $j = (c/4\pi) \text{rot } H$  from measured transversal fields becomes apparent. From the measurements of transversal fields at two levels we obtain (truly, only the first yet) indication that the flare can occur in a region where oppositely flowing currents merge (in the horizontal plane) on the "neutral" line of the electric field. These facts in general are much close to the theory of flares, developed lately by Alfvén and Carlqvist (1967) rather than to any other theory.

It was somewhat different with the second side of the problem -- variation of the magnetic fields connected with the flares, since our results from 1957 to 1957 (Severnyi, 1958 and 1960b) were subjected to doubts in 1966 by Howard and Babcock (1966) because of the example of the proton flare of importance 3+ (16 July 1959): based on the quantitative consideration of the oscilloscopic shots of the field in the region of this flare, one did not find variations in shape and location of the basic hills after its occurrence. However, the following study of 10 Crimean recordings of the fields related to the same flare from 14 to 18 July, performed by Howard and Severnyi (1963), has shown very strong variations of field and energy  $H_{\parallel}^2 V / 8\pi$  gradients (see Sec. 3), comparable to those which were observed for the flare of 7 July 1966. It turns out that all changes of gradients occurred in such a small region that is comprised of a negligible part of that resolution ( $23 \text{ arcs} \times 23 \text{ arcs}$ ), with which the field was recorded at the Mount Wilson Observatory (resolution of our recordings:  $2.5 \text{ arcs} \times 4.5 \text{ arcs}$ ). Furthermore, all field strength variations took place in the regions of high values, far exceeding that limit (100 gs) above which the Mount Wilson's recordings were located in the scale region. However, in practice simultaneously with the work of Kiepenheuer (1965), reports appeared (Evans, 1959; Chistyakov, 1959; Vasil'eva, 1961; Lerol, 1962) which substantiated the variations of magnetic fields connected with flares. In the works of Michard et al. (1961), the temporary drop of field gradients was noted and it was indicated that after the flare, the prior-to-the-flare values were re-established. On the variations of the magnetic fields of the "relaxation" type, decrease of the area occupied by the given isogauss in connection with the flares was also reported by Deubner (1965).

Finally, quite recently, a preliminary report appeared on the variation of the magnetic energy in connection with flares of the type measured by us in the works of Howard and Severnyi (1963) and Severnyi (1968). Namely, in certain active regions  $30^m$  prior to the flare, one observed the increase of the magnetic energy of the active region and its drop to the pre-flare value approximately half an hour after the flare (Rust, 1968).

Quite evident proofs of variations of the field gradients, magnetic fluxes and field energy obtained in the present work for 7 July and 2 Sept 1966 flares do not only ascertain again the results that we have obtained previously, but in our opinion, contain (mentioned first in the works of Severnyi, 1968) information on the variation of the resulting magnetic flux through the active region. These variations of the magnetic induction flux lead to the emf in the contour, surrounding the active region, of exactly that order which is actually observed in protons, generated by powerful flares. Fortunately, this result did not turn out to be unique. Simultaneously with our report (in July of 1967, COSPAR in Sept 1967, Budapest) Martres et al. (1968) have made a report which gives the example of the change of

sign of the imbalance  $F_S - F_N$  connected with the flares of 28 Sept through 5 Oct 1965. Further, when this work was completed, the work of Martres et al. (1968) was published in which the authors have qualitatively reached the same result. Based on the review of extremely abundant material – photoheliograms of groups and some isogauss maps – these authors have concluded that the flares are connected with the fact that the area (and the magnetic flux) of one of the opposite polarities increases and the other decreases. It is true that the authors cannot say anything quantitatively either on what is the flux prior to and after the flare or even what is the sign of the flux difference, since they based their work on the measurements of the area of the umbra, spot nuclei, which as is shown in Sec. 3, can lead to an incorrect (in the sense of sign and magnitude) result. However, the qualitative result of Martres et al. (1968) – variation of the flux in connection with the flare – does not raise any doubt. At the same time, for ten quiet groups, without flares, the balance of fluxes of opposite polarities is apparently quite well conserved (Stenflo, 1968), if these groups are not in the stage of development or decay.

Thus, a strong change of the magnetic induction flux through the active region is apparently one of the effects with which the flares are closely connected – effects indicating the possibility of formation of powerful emf and currents, capable of generating cosmic rays. At the same time, this effect points to the fact that in order to equate currents connected with these emf's, according to Maxwell's equation

$$\oint \text{Eds} = -\frac{1}{c} \frac{\Delta\phi}{\Delta t}, \quad j = \sigma E,$$

with these currents, which are dictated by the variations of the gradients of the field and the other basic Maxwell equation

$$j = \frac{c}{4\pi} \text{rot} H,$$

we must lower the conductivity  $c$  by  $10^2$  to  $10^3$  times, a fact which was repeatedly indicated by theoretical considerations (Schroter, 1964, Kopecky and Kuklin, 1966). With these, in the case of strong flares, the electric field intensities turn out to be an order of magnitude greater than those which are expected based on the actual measurements of velocity of motion of the solar plasma across the magnetic field  $1/c[v \times H]$  (Gopasyuk, 1964 and 1967b). In its turn, a substantial decrease of conductivity facilitates the effect of the explosion mechanism of the current column which was indicated by Alfvén and Carlqvist, (1967). One must also point attention to the fact that the densities of transversal current  $j_{\perp}$  are at least an order of

magnitude higher than those for the longitudinal fields. Therefore, the conditions of realization of the mechanism (Alfvén and Carlqvist, 1967) extend, possibly, over the photosphere region. However, the study of transversal currents, as well as that of electromagnetic force has also been started in this work and must be continued.

## Acknowledgments

The authors express their appreciation to E.P. Smirnova and E.I. Limorenko for serious assistance in analyzing recordings of the magnetic field and other data. Appreciation is extended to V.V. Gapeev for the final preparation of the drawings.

## References

- Alfvén, H., and Fälthammar, C.G. (1963) Cosmical Electrodynamics, Oxford, section 39.
- Alfvén, H., and Carlqvist, R. (1967) Solar Phys. 1:220.
- Avignon, Y., Martres, M.J., and Pick, M. Ann d'Astrophys. (1964) 27 (No. 1):23 and (1966) 29:33.
- Bruns, A.V., Nikulin, N.S., and Severnyi, A.B. (1964) Izv. Crimskoy astrofiz. obs. 33:80.
- Caroubalos, C. (1964) Ann d'Astrophys. 27 (No. 5):333.
- Chistyakov, V.N. (1959) Solnechnye dannye No. 9, 81.
- Deubner, F. (1965) Stellar a. Solar Magn. Fields, IAU Symp. No. 22, p. 369.
- Ellison M., McKenna, S., and Reid, J. (1961) Dunsink Obs. Publ. 1 (No. 3).
- Evans, J. (1959) Astron. J. 64 (No. 8):330.
- Gopasyuk, S.I. (1960) Izv. Krymskoi astrofiz. obs. 24:281.
- Gopasyuk, S.I., Ogir', M.B., Severnyi, A.B., and Shaposhnikova, E.F. (1963a) Izv. Krymskoi astrofiz. obs. 29:15.
- Gopasyuk, S.I., Ogir', M.B., and Tsap, T.T. (1963b) Izv. Krymskoi astrofiz. obs. 30:148.
- Gopasyuk, S.I. Izv. Krymskoi astrofiz. obs. (1964) 32:14 and (1967b) 38:65.
- Gopasyuk, S.I. (1967a) Izv. Krymskoi astrofiz. obs. 36:56.
- Guseinov, M.Dj. (1970) Izv. Krymskoi astrofiz. obs. 41-42:89.
- Howard, R., and Babcock, H.W. (1960) Astrophys. J. 132:218.
- Howard, R., and Severnyi, A. (1963) Astrophys. J. 137:1242.
- Kiepenheuer, K. (1965) The Solar Spectrum, D. Reidel, p. 240.
- Kopecky, M., and Kuklin, G.V. (1966) Bull. Astron. Inst. Czechosl. 17:45.
- Koval', A.N., and Stepanyan, N.N. (1970) Izv. Krymskoi astrofiz. obs. 41-42:194.

Preceding page blank

## References

- Kunzel, H. (1967) Astron. Nachr. 289:33.
- Leroi, J. Contr. a l'etude de la polar. de lun. sol., Doct. Thesis, Paris, June 1962.
- Martres, M., Michard, R., and Soru-Iscovici, I. (1966) Ann d'Astrophys. 29 (No. 3):249.
- Martres, M., Michard, R., Soru-Iscovici, I., and Tsap, T. (1968a) Structure and Development of Solar Active Regions, IAU Symp. No. 35, p. 318.
- Martres, M., Michard, R., Soru-Iscovici, I., and Tsap, T. (1968b) Solar Phys. 5:187.
- Michard, R., Mouradian, Z., and Semel, M. (1961) Ann. d'Astrophys. 24:54.
- Moreton, G.E., and Severnyi, A.B. (1968) Solar. Phys. 3:282.
- Nikulin, N.S. (1964) Izv. Krymskoi astrofiz. obs. 31:209.
- Parker, E. (1963) Astrophys. J. Suppl. Ser. 8 (No. 77):177.
- Parker, E., Summarizing talk at COSPAR Symp. on Solar Flares, Tokyo, May 1968 (in press).
- Rust, D. (1968) Astron. J. 73 (No. 5, pt. II):75.
- Schroter, E.H. (1964) Proc. Meet. on Sunspots, Florence, p. 222.
- Severnyi, A.B. Astron. M. (1956) 33 (reprint 1):74 and (1957) 34 (reprint 5):684.
- Severnyi, A.B. (1958) Izv. Krimskoi astrofiz. obs. 20:22.
- Severnyi, A.B. (1960a) Izv. Krimskoi astrofiz. obs. 24:261.
- Severnyi, A.B. (1960b) Izv. Krimskoi astrofiz. obs. 22:12.
- Severnyi, A.B., and Shabanskii, V.P. (1961) Izv. Krimskoi astrofiz. obs. 25:88.
- Severnyi, A.B. (1962a) Izv. Krimskoi astrofiz. obs. 27:71.
- Severnyi, A.B. (1962b) Astron. J. 39 (reprint 6):961.
- Severnyi, A.B. (1963) Izv. Krimskoi astrofiz. obs. 30:161.
- Severnyi, A.B. Izv. Krimskoi astrofiz. obs. (1964a) 31:126 and (1965a) 33:3.
- Severnyi, A.B. (1964b) Izv. Krimskoi astrofiz. obs. 31:159.
- Severnyi, A.B. (1965b) Izv. Krimskoi astrofiz. obs. 33:34.
- Severnyi, A.B. (1966) Astron. J. 43 (print 3):465.
- Severnyi, A.B. (1967) Izv. Krimskoi astrofiz. obs. 36:22.
- Severnyi, A.B. (1968) Annals of the IQSY 3:182.
- Smith, S., and Ramsey, H. (1967) Solar Phys. 2 (No. 2):158.
- Stenflo, J.O. (1968) Structure and Development of Solar Active Regions, IAU Symp. No. 35, p. 47.
- Steshenko, N.V. (1968) Structure and Development of Solar Active Regions, IAU Symp. No. 35, p. 201.
- Sweet, P. (1958) Electromagnetic Phenomena in Cosmical Physics, IAU Symp. No. 6, p. 123.

## References

- Syrovatskii, S.I. (1966) JETF 50:113.
- Syrovatskii, S.I., COSPAR Symposium on Solar Flares, Tokyo, May 1968 (in press).
- Tandberg-Hanssen, E., and McKim Malville, J. (1968) Astron. J. 73 (No. 5, pt. II):69.
- Vasil'eva, G.Ya. (1961) Solnechnie dannie No. 12:64.
- Wentzel, D. (1964) Astrophys. J. 140:1563.